

---

# OBJECT TRACKING INCORPORATING TRANSFER LEARNING INTO UNSCENTED AND CUBATURE KALMAN FILTERS

---

A PREPRINT

Omar Alotaibi and Brian L. Mark \*

August 15, 2024

## ABSTRACT

We present a novel filtering algorithm that employs Bayesian transfer learning to address the challenges posed by mismatched intensity of the noise in a pair of sensors, each of which tracks an object using a nonlinear dynamic system model. In this setting, the primary sensor experiences a higher noise intensity in tracking the object than the source sensor. To improve the estimation accuracy of the primary sensor, we propose a framework that integrates Bayesian transfer learning into an unscented Kalman filter (UKF) and a cubature Kalman filter (CKF). In this approach, the parameters of the predicted observations in the source sensor are transferred to the primary sensor and used as an additional prior in the filtering process. Our simulation results show that the transfer learning approach significantly outperforms the conventional isolated UKF and CKF. Comparisons to a form of measurement vector fusion are also presented.

**Keywords** Object tracking, nonlinear model, Bayesian transfer learning, unscented Kalman filter, cubature Kalman filter, numerical instability.

## 1 Introduction

Tracking models of dynamic systems have been widely used in applications where achieving high estimation accuracy is critical. Bayesian filters are often used in such applications, although optimal solutions do not exist for tracking nonlinear models [2]. The unscented Kalman filter (UKF), introduced in [3], is a suboptimal Bayesian filter for nonlinear model tracking that relies on a Gaussian assumption based on a set of sigma points drawn using the unscented transformation (UT). In [4], another approximate filter for nonlinear models, the cubature Kalman filter (CKF), was proposed, based on the third-degree cubature rule to achieve better accuracy and numerical stability. While the characteristics of the UKF and CKF in isolation have been well-studied, relatively little work has been done on the application of such filters in scenarios with multiple sensors. Moreover, in multi-sensor scenarios, it is often assumed that all sensors operate under the same environmental conditions. In practice, this assumption may not always be valid because each sensor may encounter varying conditions, resulting in variations in the accuracy of the estimation among sensors. To ameliorate such conditions, sensors may collaborate by sharing information with one another.

In this paper, we consider a two-sensor system in which both sensors track an object using a UKF or CKF while experiencing different noise intensities. We designate one of the sensors as the source sensor and the other as the primary sensor. We shall assume that the primary sensor experiences higher noise intensity than the source sensor. To improve the estimation accuracy of the primary sensor, the source sensor shares the outcome of the source tracking task instead of the raw data from the source domain. This is an example of what is known in the machine learning literature as transfer learning [5].

Transfer learning has been successfully used to address filtering sparsity problems [6, 7]. Bayesian models have been used in transfer learning approaches for probabilistic graphical models, such as sharing a Gaussian prior [8]. The incorporation of transfer learning with Bayesian approaches to improve the performance of the target domain

---

\*A preliminary version of this work was presented in [1]. The authors are with the Department of Electrical and Computer Engineering, George Mason University, Fairfax, VA 22030 USA (e-mail: oalotaib@gmu.edu; bmark@gmu.edu).

is referred to as Bayesian transfer learning (BTL) [9, 10]. In [11, 12], BTL was used to model the interacting tasks of Gaussian process regression. Moreover, transfer learning has been paired with a Bayesian inference framework to transfer a visual prior learned for online object tracking in challenging environments [13]. In [14–16], BTL was applied in the context of a two-sensor system with mismatched noise intensities in which each sensor employs a Kalman filter to track a linear motion model of an object. The source sensor shares its predicted observations to improve the estimation performance of the primary sensor.

Our work extends the BTL approach referred to as fully probabilistic design (FPD) in [14] to the case of tracking a *nonlinear* model of a dynamical system with the UKF and CKF. In particular, we adopt the FPD variant approach of [14], in which both the mean and covariance of the *predicted* observations of the source sensor are transferred to the primary sensor, rather than the observed raw measurement data [5]. The size of the predicted observation data is significantly smaller than the raw, cluttered observed data from the source domain [11], which are used in the traditional measurement vector fusion (MVF) approach to multi-sensor fusion [17]. Furthermore, sharing the predicted observations is superior from a security prospective, since the raw observations may carry information that may be undesirable for the source to disclose.

The main contributions of our work are two-fold: (1) We formulate a new BTL approach for tracking a nonlinear model using the UKF or CKF in a two-sensor system. (2) Our simulation results reveal new insights into the performance and numerical stability of the UKF and CKF in a multi-sensor system with knowledge sharing between sensors. Our simulation results show significant gains in estimation accuracy of the proposed tracking framework compared to the isolated UKF or CKF. An interesting observation is that the UKF integrated with BTL, referred to as transfer learning-unscented Kalman filter (TL-UKF), is more sensitive to the value of the UKF parameter  $\kappa$  than the isolated UKF. In particular, as  $\kappa$  is increased, the improvement in the performance of TL-UKF is greater than that of the isolated UKF. Similarly, increasing the cubature degree of the CKF from three (equivalent to UKF with  $\kappa = 0$ ) to five results in a greater performance gain of transfer learning-cubature Kalman filter (TL-CKF) relative to the isolated CKF. Furthermore, integrating BTL into UKF, third-degree CKF, fifth-degree CKF outperforms not only the estimation accuracy of the isolated filters, it also performs slightly better than MVF [17], which is known to outperform other fusion approaches for multi-sensor systems such as state vector fusion [18].

The remainder of the paper is organized as follows. In Section 2, we provide a brief overview of the state-space representation and the traditional Bayesian filtering approach for object tracking in a two-sensor system with mismatched intensity levels of measurement noise. Section 3 introduces the BTL framework for tracking a nonlinear dynamic system model using two sensors. Section 4 derives the Gaussian process resulting from incorporating BTL into the Bayesian filtering approach under the Gaussian assumption. Section 5 discusses the proposed tracking algorithm that integrates transfer learning into the UKF in the source and primary sensors. Section 6 addresses the numerical instability issue in the UKF. Section 7 addresses integration of transfer learning into the third-degree and fifth-degree CKF. Simulation results for the proposed algorithm are presented in Section 8. The paper is concluded in Section 9.

## 2 System Model

### 2.1 State Space Representation

The discrete-time state space representation (SSR) for describing the dynamics of a general dynamical system is given as follows:

$$\mathbf{x}_k = f_k(\mathbf{x}_{k-1}) + \mathbf{v}_{k-1} \quad (1)$$

$$\mathbf{z}_k = h_k(\mathbf{x}_k) + \mathbf{w}_k \quad (2)$$

where  $k \in \mathbb{N}$  denotes the discrete time step. The vector  $\mathbf{x}_k \in \mathbb{R}^{n_x}$  represents the state of the system at time step  $k$  with a dimension of  $n_x$ . The function  $f_k : \mathbb{R}^{n_x} \rightarrow \mathbb{R}^{n_x}$  is the dynamic transition function, which describes how the state evolves over time. The vector  $\mathbf{z}_k \in \mathbb{R}^{n_z}$  represents the measurements obtained from the system at time step  $k$  with a dimension of  $n_z$ . The function  $h_k : \mathbb{R}^{n_x} \rightarrow \mathbb{R}^{n_z}$  is the measurement function that relates the state to the measurements. The variables  $\mathbf{v}_{k-1} \in \mathbb{R}^{n_v}$  and  $\mathbf{w}_k \in \mathbb{R}^{n_w}$  correspond to the process noise and measurement noise with dimensions of  $n_v$  and  $n_w$ , respectively, representing the uncertainties and disturbances in the system [19]. The state and measurement noises are assumed to be independent and identically distributed (i.i.d.) zero-mean Gaussian random vector sequences characterized by

$$\mathbf{v}_{k-1} \stackrel{\text{iid}}{\sim} \mathcal{N}(\mathbf{0}, \mathbf{Q}_v), \quad \mathbf{w}_k \stackrel{\text{iid}}{\sim} \mathcal{N}(\mathbf{0}, \mathbf{Q}_w), \quad (3)$$

respectively, where  $\mathbf{Q}_v$  and  $\mathbf{Q}_w$  denote the covariance matrices.

## 2.2 Bayesian Filter Approach

In the Bayesian filter approach, the posterior probability density function (PDF) of the state is constructed by incorporating all available statistical information and the sequence of observations. The extraction of the estimated state from the posterior PDF provides an optimal solution to address the estimation problem [20, 21]. The estimation of the state  $\mathbf{x}_k$  within the Bayesian filter approach is conducted through a two-step process:

- **Prediction Step:** The computation of the prediction for the posterior PDF of the next state  $\mathbf{x}_k$  at time step  $k$ , given the set of measurements up to time step  $k-1$ , denoted as  $\mathbf{z}_{1:k-1} = \{\mathbf{z}_1, \dots, \mathbf{z}_{k-1}\}$ , is performed using the Chapman-Kolmogorov equation [19, 20, 22]. This equation provides a framework for recursively updating the PDF based on the available information up to the previous time step as follows:

$$p(\mathbf{x}_k | \mathbf{z}_{1:k-1}) = \int_{\mathbb{R}^{n_x}} p(\mathbf{x}_k | \mathbf{x}_{k-1}) p(\mathbf{x}_{k-1} | \mathbf{z}_{1:k-1}) d\mathbf{x}_{k-1}, \quad (4)$$

where  $p(\mathbf{x}_{k-1} | \mathbf{z}_{1:k-1})$  is the posterior density of the state at the previous time step  $k-1$  and  $p(\mathbf{x}_k | \mathbf{x}_{k-1})$  is the transitioning PDF characterized by (1).

- **Update Step:** The updated posterior PDF for  $\mathbf{x}_k$  given  $\mathbf{z}_{1:k}$  is obtained by applying Bayes' rule immediately after the new measurement at time step  $k$  is observed [22]. This process incorporates the most recent measurement information into the estimation process, resulting in an improved representation of the state's posterior density as

$$p(\mathbf{x}_k | \mathbf{z}_{1:k}) = \frac{p(\mathbf{z}_k | \mathbf{x}_k) p(\mathbf{x}_k | \mathbf{z}_{1:k-1})}{p(\mathbf{z}_k | \mathbf{z}_{1:k-1})}, \quad (5)$$

where  $p(\mathbf{z}_k | \mathbf{x}_k)$  is the measurement likelihood density function, as described in (2), at time step  $k$ . Furthermore, the normalization factor  $p(\mathbf{z}_k | \mathbf{z}_{1:k-1})$  is given by

$$p(\mathbf{z}_k | \mathbf{z}_{1:k-1}) = \int_{\mathbb{R}^{n_x}} p(\mathbf{z}_k | \mathbf{x}_k) p(\mathbf{x}_k | \mathbf{z}_{1:k-1}) d\mathbf{x}_k, \quad (6)$$

The state and measurement models described by (1) and (2) are Gaussian processes due to the assumption of Gaussian noise sources as given by (3). The Gaussian process assumption leads to a posterior density for the state that is also Gaussian, characterized by its mean and covariance. Consequently, the recursive nature of the Bayesian filter approach primarily revolves around the updates of means and covariances of conditional densities over time and measurements. The two main steps of the Bayesian filter approach, the prediction and update steps, can be reformulated under the assumption of a Gaussian process.

## 2.3 Tracking with Mismatched Noise Intensities

We consider the problem of estimating an unknown state  $\mathbf{x}_k$  at time step  $k$ , assuming a state transition model defined by

$$\mathbf{x}_k = f(\mathbf{x}_{k-1}) + \mathbf{v}_{k-1} \implies p(\mathbf{x}_k | \mathbf{x}_{k-1}), \quad (7)$$

where  $f(\cdot)$  denotes the state transition function and  $\mathbf{v}_{k-1}$  represents the error process, which is assumed to be zero-mean additive white Gaussian noise (AWGN) with covariance matrix  $\mathbf{Q}_v$ . At each time step, an estimator filter with its own sensor observes measurements  $\mathbf{z}_k$  that are associated with the desired object. The observable measurements are modeled via

$$\mathbf{z}_k = h(\mathbf{x}_k) + \mathbf{w}_k \implies p(\mathbf{z}_k | \mathbf{x}_k), \quad (8)$$

where  $h(\cdot)$  provides a representation of the measurement parameters of the unknown state parameters. The measurement noise  $\mathbf{w}_k$  is assumed to be Gaussian with covariance matrix  $\mathbf{Q}_w = I_w \mathbf{B}_w$ .

In this paper, we consider a two-sensor system in which the observed measurements have mismatched noise intensities  $I_w$  between the sensors due to various environmental or technical factors that affect the observable measurements. This leads to a reduction in estimation accuracy of the impacted tracking system. In the two-sensor system, we shall denote the quantities associated with the source sensor with a superscript  $\star$  and those associated with the primary sensor without a superscript. Each sensor tracks the same moving object as illustrated in Fig. 1 where both sensors are affected by noise with intensities, denoted by  $I_w^\star$  and  $I_w$ , corresponding to the source and primary sensors, respectively.

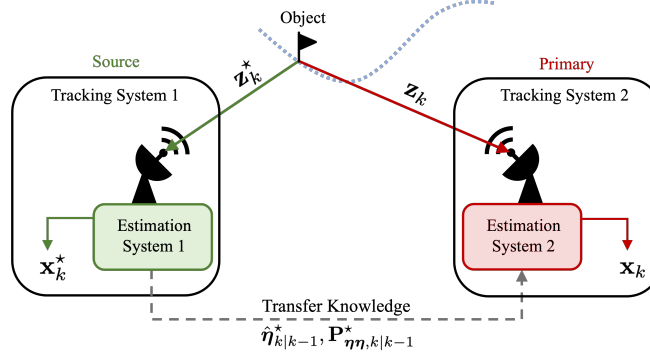


Figure 1: Graphical illustration of knowledge transfer between source and primary sensors tracking the same moving object.

### 3 Bayesian Transfer Learning Filter Approach

We apply BTL to incorporate knowledge shared from the source to the primary tracking filter [8, 9]. This integration of BTL within the tracking filter framework is referred to as Bayesian transfer learning filter (BTLF). In particular, the source sensor shares its predicted observations with the primary sensor. This approach is applicable in scenarios where a system observes limited or unreliable measurements due to adverse conditions, such as high levels of noise intensity.

#### 3.1 Source Tracking Filter

The source filter comprises an unknown state variable set  $\mathbf{x}^* = \{\mathbf{x}_1^*, \dots, \mathbf{x}_K^*\}$  and an observable measurement variable set  $\mathbf{z}^* = \{\mathbf{z}_1^*, \dots, \mathbf{z}_K^*\}$ . Unlike the conventional Bayesian approach, the predicted observation variable set  $\boldsymbol{\eta}^* = \{\boldsymbol{\eta}_2^*, \dots, \boldsymbol{\eta}_{K+1}^*\}$  is introduced into the BTLF. The overall posterior density of the state object and predicted observation  $p(\mathbf{x}_k^*, \boldsymbol{\eta}_{k+1}^* | \mathbf{z}_{1:k}^*)$ , given the measurements set up to time step  $k$ , denoted as  $\mathbf{z}_{1:k}^* = \{\mathbf{z}_1^*, \dots, \mathbf{z}_k^*\}$ , can be estimated by the product of two posterior densities, which are derived in Appendix B:

$$p(\mathbf{x}_k^*, \boldsymbol{\eta}_{k+1}^* | \mathbf{z}_{1:k}^*) \propto p(\mathbf{x}_k^* | \boldsymbol{\eta}_{k+1}^*, \mathbf{z}_{1:k}^*) p(\boldsymbol{\eta}_{k+1}^* | \mathbf{z}_{1:k}^*). \quad (9)$$

Since, the object state  $\mathbf{x}_k^*$  at the current time step  $k$  is conditionally independent of the predicted observation variable  $\boldsymbol{\eta}_{k+1}^*$  for the next time step  $k+1$ , the conditional probability  $p(\mathbf{x}_k^* | \boldsymbol{\eta}_{k+1}^*, \mathbf{z}_{1:k}^*)$  in (9) can be simplified to  $p(\mathbf{x}_k^* | \mathbf{z}_{1:k}^*)$ . The posterior density of the object state  $p(\mathbf{x}_k^* | \mathbf{z}_{1:k}^*)$  can be expressed as

$$p(\mathbf{x}_k^* | \mathbf{z}_{1:k}^*) \propto p(\mathbf{z}_k^* | \mathbf{x}_k^*) p(\mathbf{x}_k^* | \mathbf{x}_{k-1}^*) p(\mathbf{x}_{k-1}^* | \mathbf{z}_{1:k-1}^*), \quad (10)$$

where  $p(\mathbf{z}_k^* | \mathbf{x}_k^*)$  represents the measurement likelihood function, and  $p(\mathbf{x}_k^* | \mathbf{x}_{k-1}^*)$  denotes the predicted state for the next time step, computed using the transition PDF given in (7). Upon obtaining the estimated object state  $\mathbf{x}_k^*$  from (10), the posterior density of the predicted observation  $p(\boldsymbol{\eta}_{k+1}^* | \mathbf{z}_{1:k}^*)$  as described in (9) can be estimated by

$$p(\boldsymbol{\eta}_{k+1}^* | \mathbf{z}_{1:k}^*) \propto p(\boldsymbol{\eta}_{k+1}^* | \mathbf{x}_{k+1}^*) p(\mathbf{x}_{k+1}^* | \mathbf{x}_k^*) p(\mathbf{x}_k^* | \mathbf{z}_{1:k}^*), \quad (11)$$

where  $p(\boldsymbol{\eta}_{k+1}^* | \mathbf{x}_{k+1}^*)$  follows the measurement density model described in (8). Estimation of the overall posterior density of the state object and the predicted observation, denoted as  $p(\mathbf{x}_k^*, \boldsymbol{\eta}_{k+1}^* | \mathbf{z}_{1:k}^*)$  in (9), is achieved using a three-step process:

- **Prediction Step:** The predictive density of the object state can be computed by applying (4) in the traditional Bayesian approach as follows:

$$p(\mathbf{x}_k^* | \mathbf{z}_{1:k-1}^*) = \int_{\mathbb{R}^{n_x}} p(\mathbf{x}_k^* | \mathbf{x}_{k-1}^*) p(\mathbf{x}_{k-1}^* | \mathbf{z}_{1:k-1}^*) d\mathbf{x}_{k-1}^*. \quad (12)$$

- **Update Step:** The state posterior density is updated using Bayes' rule, as described by (5) and (6), yielding the following expression:

$$p(\mathbf{x}_k^* | \mathbf{z}_{1:k}^*) = \frac{p(\mathbf{z}_k^* | \mathbf{x}_k^*) p(\mathbf{x}_k^* | \mathbf{z}_{1:k-1}^*)}{p(\mathbf{z}_k^* | \mathbf{z}_{1:k-1}^*)}, \quad (13)$$

where  $p(\mathbf{z}_k^* | \mathbf{z}_{1:k-1}^*)$  is defined as

$$p(\mathbf{z}_k^* | \mathbf{z}_{1:k-1}^*) = \int_{\mathbb{R}^{n_x}} p(\mathbf{z}_k^* | \mathbf{x}_k^*) p(\mathbf{x}_k^* | \mathbf{z}_{1:k-1}^*) d\mathbf{x}_k^* \quad (14)$$

The second term  $p(\boldsymbol{\eta}_{k+1}^* | \mathbf{z}_{1:k}^*)$  in (109) represents the posterior density of the predicted observation, which is estimated in the next step.

• **Predict Observation Step:** The predicted observation density can be computed using (4) and (6) as follows:

$$p(\boldsymbol{\eta}_{k+1}^* | \mathbf{z}_{1:k}^*) = \int_{\mathbb{R}^{n_x}} p(\boldsymbol{\eta}_{k+1}^* | \mathbf{x}_{k+1}^*) p(\mathbf{x}_{k+1}^* | \mathbf{z}_{1:k}^*) d\mathbf{x}_{k+1}^* \quad (15)$$

where  $p(\mathbf{x}_{k+1}^* | \mathbf{z}_{1:k}^*)$  represents the predictive density at time step  $k + 1$ , given the set of measurements up to time step  $k$ , which is defined by

$$p(\mathbf{x}_{k+1}^* | \mathbf{z}_{1:k}^*) = \int_{\mathbb{R}^{n_x}} p(\mathbf{x}_{k+1}^* | \mathbf{x}_k^*) p(\mathbf{x}_k^* | \mathbf{z}_{1:k}^*) d\mathbf{x}_k^*. \quad (16)$$

### 3.2 Primary Tracking Filter

The predicted observations,  $\boldsymbol{\eta}_{2:k}^*$ , from the source tracking filter, are transferred and used simultaneously as prior knowledge to estimate a set of object state variables  $\mathbf{x} = \{\mathbf{x}_1, \dots, \mathbf{x}_K\}$  under different conditions in the primary tracking filter given a set of measurement variables  $\mathbf{z} = \{\mathbf{z}_1, \dots, \mathbf{z}_K\}$ . By applying the BTLF into the primary tracking system, the overall posterior density of the object state given the transferred predicted observations  $\boldsymbol{\eta}_{2:k}^*$  and the observed measurements  $\mathbf{z}_{1:k}$  up to time step  $k$  is estimated as follows:

$$p(\mathbf{x}_k | \mathbf{z}_{1:k}, \boldsymbol{\eta}_{2:k}^*) \propto p(\mathbf{z}_k | \mathbf{x}_k, \mathbf{z}_{1:k-1}, \boldsymbol{\eta}_{2:k}^*) p(\mathbf{x}_k | \mathbf{z}_{1:k-1}, \boldsymbol{\eta}_{2:k}^*). \quad (17)$$

The transfer learning framework's state posterior density, denoted as  $p(\mathbf{x}_k | \mathbf{z}_{1:k-1}, \boldsymbol{\eta}_{2:k}^*)$  is computed via Bayes' rule:

$$p(\mathbf{x}_k | \mathbf{z}_{1:k-1}, \boldsymbol{\eta}_{2:k}^*) \propto p(\boldsymbol{\eta}_k^* | \mathbf{x}_k, \mathbf{z}_{1:k-1}, \boldsymbol{\eta}_{2:k-1}^*) p(\mathbf{x}_k | \mathbf{x}_{k-1}). \quad (18)$$

Under the assumption that the measurement at the current time step  $k$  is conditionally independent of all previous measurements, given the current state  $\mathbf{x}_k$ , and that the measurements  $\mathbf{z}$  and the transferred predicted observations  $\boldsymbol{\eta}^*$  are independent, conditioned on the current state  $\mathbf{x}_k$ , the overall state posterior can be simplified and obtained by substituting the transfer learning state posterior from (18) into (17):

$$p(\mathbf{x}_k | \mathbf{z}_{1:k}, \boldsymbol{\eta}_{2:k}^*) \propto p(\mathbf{z}_k | \mathbf{x}_k) p(\boldsymbol{\eta}_k^* | \mathbf{x}_k) p(\mathbf{x}_k | \mathbf{x}_{k-1}). \quad (19)$$

Appendix B provides a proof of the estimation procedure for the overall posterior density, as described in (19), which involves two distinct likelihood functions: the transferred predicted observation likelihood function  $p(\boldsymbol{\eta}_k^* | \mathbf{x}_k)$  and the measurement likelihood function  $p(\mathbf{z}_k | \mathbf{x}_k)$ . By incorporating the transferred knowledge of the predicted observation, the overall posterior density can be estimated, which leads to enhanced accuracy in the object state estimation process, through the following two-step procedure:

• **Prediction Step:** The prediction density of object state given measurements and transferred predicted observation up to previous time step  $k - 1$  can be obtained, following (4), as

$$p(\mathbf{x}_k | \mathbf{z}_{1:k-1}, \boldsymbol{\eta}_{1:k-1}^*) = \int_{\mathbb{R}^{n_x}} p(\mathbf{x}_k | \mathbf{x}_{k-1}) p(\mathbf{x}_{k-1} | \mathbf{z}_{1:k-1}, \boldsymbol{\eta}_{1:k-1}^*) d\mathbf{x}_{k-1}. \quad (20)$$

• **Update Step:** The state posterior density is updated using two likelihood functions

$$p(\mathbf{x}_k | \mathbf{z}_{1:k-1}, \boldsymbol{\eta}_{1:k}^*) = \frac{p(\boldsymbol{\eta}_k^* | \mathbf{x}_k) p(\mathbf{x}_k | \mathbf{z}_{1:k-1}, \boldsymbol{\eta}_{1:k-1}^*)}{p(\boldsymbol{\eta}_k^* | \mathbf{z}_{1:k-1}, \boldsymbol{\eta}_{1:k-1}^*)}, \quad (21)$$

$$p(\mathbf{x}_k | \mathbf{z}_{1:k}, \boldsymbol{\eta}_{1:k}^*) = \frac{p(\mathbf{z}_k | \mathbf{x}_k) p(\mathbf{x}_k | \mathbf{z}_{1:k-1}, \boldsymbol{\eta}_{1:k}^*)}{p(\mathbf{z}_k | \mathbf{z}_{1:k-1}, \boldsymbol{\eta}_{1:k}^*)}, \quad (22)$$

where the denominators in (21) and (22), respectively, are defined according to (6) as

$$p(\boldsymbol{\eta}_k^* | \mathbf{z}_{1:k-1}, \boldsymbol{\eta}_{1:k-1}^*) = \int_{\mathbb{R}^{n_x}} p(\boldsymbol{\eta}_k^* | \mathbf{x}_k) p(\mathbf{x}_k | \mathbf{z}_{1:k-1}, \boldsymbol{\eta}_{1:k-1}^*) d\mathbf{x}_k, \quad (23)$$

$$p(\mathbf{z}_k | \mathbf{z}_{1:k-1}, \boldsymbol{\eta}_{1:k}^*) = \int_{\mathbb{R}^{n_x}} p(\mathbf{z}_k | \mathbf{x}_k) p(\mathbf{x}_k | \mathbf{z}_{1:k-1}, \boldsymbol{\eta}_{1:k}^*) d\mathbf{x}_k. \quad (24)$$

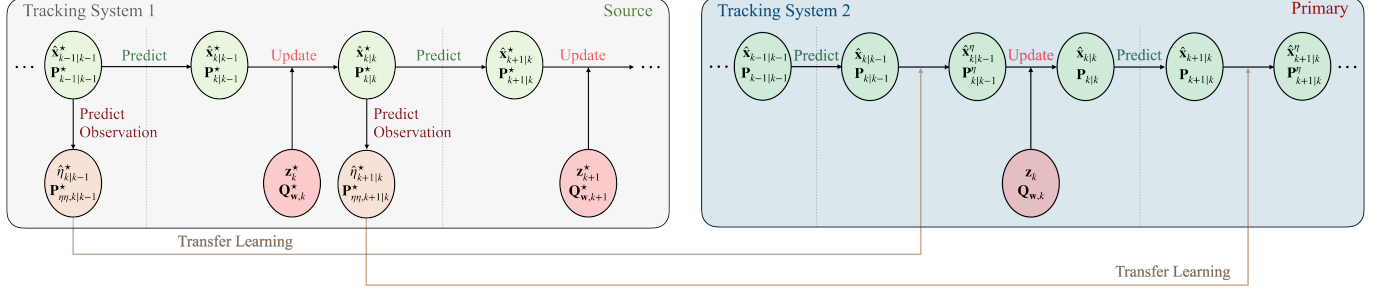


Figure 2: Visual depiction of the BTLF procedure, illustrating the source and primary filters and the transfer of knowledge between these filters.

## 4 Gaussian Process of Bayesian Transfer Learning Filter Approach

In the BTLF approach, the predictive density,  $p(\mathbf{x}_k | \mathbf{x}_{k-1})$ , the measurement likelihood density,  $p(\mathbf{z}_k | \mathbf{x}_k)$ , and the transferred predicted observation likelihood density,  $p(\boldsymbol{\eta}_k^* | \mathbf{x}_k)$ , follow Gaussian distributions. This is due to the assumption that the state and measurement noises in the state space models given by (1) and (2) are Gaussian, as described in (3). Therefore, this assumption leads to a Gaussian posterior density [4, 21]. Under this Gaussian assumption, the BTLF approach can be refined to recursively update the mean and covariance of the conditional densities over time, measurements, and transferred parameters. Fig. 2 illustrates the procedure of both the source and primary tracking filters, incorporating a transfer learning approach between these two tracking filters.

### 4.1 Source Tracking Filter

The overall posterior of the state and the predicted observation can be estimated through three steps: prediction, update, and predict observation steps, as follows:

- **Prediction Step:** The predictive density of the object state in (12) is represented as a Gaussian density,  $p(\mathbf{x}_k^* | \mathbf{z}_{1:k-1}^*) = \mathcal{N}(\hat{\mathbf{x}}_k^*; \hat{\mathbf{x}}_{k|k-1}^*, \mathbf{P}_{k|k-1}^*)$ , where  $\hat{\mathbf{x}}_{k|k-1}^*$  is the mean of the predictive density and  $\mathbf{P}_{k|k-1}^*$  is the covariance matrix. Under the assumption of zero-mean Gaussian process noise that is independent of previous measurements, the mean of the predictive density can be computed as follows:

$$\hat{\mathbf{x}}_{k|k-1}^* = E[\mathbf{x}_k^* | \mathbf{z}_{1:k-1}^*] = \int_{\mathbb{R}^{n_x}} f_k(\mathbf{x}_{k-1}^*) p(\mathbf{x}_{k-1}^* | \mathbf{z}_{1:k-1}^*) d\mathbf{x}_{k-1}^*. \quad (25)$$

The associated covariance matrix  $\mathbf{P}_{k|k-1}^*$  of the predictive Gaussian density can be obtained as

$$\mathbf{P}_{k|k-1}^* = E[(\mathbf{x}_k^* - \hat{\mathbf{x}}_{k|k-1}^*) (\mathbf{x}_k^* - \hat{\mathbf{x}}_{k|k-1}^*)^T | \mathbf{z}_{1:k-1}^*] \quad (26)$$

$$= \int_{\mathbb{R}^{n_x}} f_k(\mathbf{x}_{k-1}^*) (f_k(\mathbf{x}_{k-1}^*))^T p(\mathbf{x}_{k-1}^* | \mathbf{z}_{1:k-1}^*) d\mathbf{x}_{k-1}^* - \hat{\mathbf{x}}_{k|k-1}^* (\hat{\mathbf{x}}_{k|k-1}^*)^T + \mathbf{Q}_{w,k}^*. \quad (27)$$

- **Update Step:** Under the assumption of independent zero-mean Gaussian measurement noise, the predictive observation  $p(\mathbf{z}_k^* | \mathbf{z}_{1:k-1}^*)$  described in (14) follows a Gaussian distribution. The mean  $\hat{\mathbf{z}}_{k|k-1}^*$  and covariance  $\mathbf{P}_{\mathbf{z}\mathbf{z},k|k-1}^*$  of this distribution can be computed via the following equations:

$$\begin{aligned} \hat{\mathbf{z}}_{k|k-1}^* &= E[\mathbf{z}_k^* | \mathbf{z}_{1:k-1}^*] \\ &= \int_{\mathbb{R}^{n_x}} h_k(\mathbf{x}_k^*) p(\mathbf{x}_k^* | \mathbf{z}_{1:k-1}^*) d\mathbf{x}_k^* \end{aligned} \quad (28)$$

and

$$\begin{aligned} \mathbf{P}_{\mathbf{z}\mathbf{z},k|k-1}^* &= E[(\mathbf{z}_k^* - \hat{\mathbf{z}}_{k|k-1}^*) (\mathbf{z}_k^* - \hat{\mathbf{z}}_{k|k-1}^*)^T | \mathbf{z}_{1:k-1}^*] \\ &= \int_{\mathbb{R}^{n_x}} h_k(\mathbf{x}_k^*) (h_k(\mathbf{x}_k^*))^T p(\mathbf{x}_k^* | \mathbf{z}_{1:k-1}^*) d\mathbf{x}_k^* - \hat{\mathbf{z}}_{k|k-1}^* (\hat{\mathbf{z}}_{k|k-1}^*)^T + \mathbf{Q}_{w,k}^*, \end{aligned} \quad (29)$$

where the cross-covariance of between the state and the measurement, denoted as  $\mathbf{P}_{\mathbf{x}\mathbf{z},k|k-1}^*$ , can be obtained as

$$\begin{aligned} \mathbf{P}_{\mathbf{x}\mathbf{z},k|k-1}^* &= E[(\mathbf{x}_k^* - \hat{\mathbf{x}}_{k|k-1}^*) (\mathbf{z}_k^* - \hat{\mathbf{z}}_{k|k-1}^*)^T | \mathbf{z}_{1:k-1}^*] \\ &= \int_{\mathbb{R}^{n_x}} \mathbf{x}_k^* (h_k(\mathbf{x}_k^*))^T p(\mathbf{x}_k^* | \mathbf{z}_{1:k-1}^*) d\mathbf{x}_k^* - \hat{\mathbf{x}}_{k|k-1}^* (\hat{\mathbf{z}}_{k|k-1}^*)^T. \end{aligned} \quad (30)$$

Once the new observed measurement arrives at time  $k$ , the posterior density of the state, as defined in Equation (13), follows a Gaussian distribution, given by  $p(\mathbf{x}_k^* | \mathbf{z}_{1:k}^*) = \mathcal{N}(\mathbf{x}_k^*; \hat{\mathbf{x}}_{k|k}^*, \mathbf{P}_{k|k}^*)$ . The mean and covariance of this density, denoted as  $\hat{\mathbf{x}}_{k|k}^*$  and  $\mathbf{P}_{k|k}^*$  respectively, can be calculated using the following procedure:

$$\hat{\mathbf{x}}_{k|k}^* = \hat{\mathbf{x}}_{k|k-1}^* + \mathbf{K}_k^* (\mathbf{z}_k^* - \hat{\mathbf{z}}_{k|k-1}^*), \quad (31)$$

$$\mathbf{P}_{k|k}^* = \mathbf{P}_{k|k-1}^* - \mathbf{K}_k^* \mathbf{P}_{\mathbf{z}\mathbf{z},k|k-1}^* (\mathbf{K}_k^*)^T, \quad (32)$$

where  $\mathbf{K}_k^*$  is a linear gain given by

$$\mathbf{K}_k^* = \mathbf{P}_{\mathbf{x}\mathbf{z},k|k-1}^* (\mathbf{P}_{\mathbf{z}\mathbf{z},k|k-1}^*)^{-1}. \quad (33)$$

• **Predicted Observation Step:** The predicted observation density in (15) is modeled as a Gaussian distribution, expressed as  $p(\boldsymbol{\eta}_{k+1}^* | \mathbf{z}_{1:k}^*) = \mathcal{N}(\boldsymbol{\eta}_{k+1}^*; \hat{\boldsymbol{\eta}}_{k+1|k}^*, \mathbf{P}_{\boldsymbol{\eta}\boldsymbol{\eta},k+1|k}^*)$ . In this representation, the mean of the density,  $\hat{\boldsymbol{\eta}}_{k+1|k}^*$ , and the covariance matrix,  $\mathbf{P}_{\boldsymbol{\eta}\boldsymbol{\eta},k+1|k}^*$ , are computed via

$$\begin{aligned} \hat{\boldsymbol{\eta}}_{k+1|k}^* &= E[\boldsymbol{\eta}_{k+1}^* | \mathbf{z}_{1:k}^*] = E[\mathbf{z}_{k+1}^* | \mathbf{z}_{1:k}^*] = \hat{\mathbf{z}}_{k+1|k}^* \\ &= \int_{\mathbb{R}^{n_{\mathbf{x}}}} h_k(\mathbf{x}_{k+1}^*) p(\mathbf{x}_{k+1}^* | \mathbf{z}_{1:k}^*) d\mathbf{x}_{k+1}^*, \end{aligned} \quad (34)$$

and

$$\begin{aligned} \mathbf{P}_{\boldsymbol{\eta}\boldsymbol{\eta},k+1|k}^* &= E[(\boldsymbol{\eta}_{k+1}^* - \hat{\boldsymbol{\eta}}_{k+1|k}^*) (\boldsymbol{\eta}_{k+1}^* - \hat{\boldsymbol{\eta}}_{k+1|k}^*)^T | \mathbf{z}_{1:k}^*] \\ &= \int_{\mathbb{R}^{n_{\mathbf{x}}}} h_k(\mathbf{x}_{k+1}^*) (h_k(\mathbf{x}_{k+1}^*))^T p(\mathbf{x}_{k+1}^* | \mathbf{z}_{1:k}^*) d\mathbf{x}_{k+1}^* - \hat{\boldsymbol{\eta}}_{k+1|k}^* (\hat{\boldsymbol{\eta}}_{k+1|k}^*)^T + \mathbf{Q}_{\mathbf{w},k}^*, \end{aligned} \quad (35)$$

where the mean of the predictive density,  $p(\mathbf{x}_{k+1}^* | \mathbf{z}_{1:k}^*)$ , is computed by

$$\hat{\mathbf{x}}_{k+1|k}^* = E[\mathbf{x}_{k+1}^* | \mathbf{z}_{1:k}^*] = \int_{\mathbb{R}^{n_{\mathbf{x}}}} f_k(\mathbf{x}_k^*) p(\mathbf{x}_k^* | \mathbf{z}_{1:k}^*) d\mathbf{x}_k^*. \quad (36)$$

Note that the mean and covariance of the predicted observation density  $p(\boldsymbol{\eta}_{k+1}^* | \mathbf{z}_{1:k}^*)$  in (34) and (35) are the same parameters of the predicted observation  $p(\mathbf{z}_{k+1}^* | \mathbf{z}_{1:k}^*)$  with associated mean  $\hat{\mathbf{z}}_{k+1|k}^*$  and covariance  $\mathbf{P}_{\mathbf{z}\mathbf{z},k+1|k}^*$  computed in (28) and (29). Thus, this approach does not require any additional computational process time in the source tracking filter. Upon estimating the density parameters,  $(\hat{\boldsymbol{\eta}}_{k+1|k}^*, \mathbf{P}_{\boldsymbol{\eta}\boldsymbol{\eta},k+1|k}^*)$ , which characterize the Gaussian distribution of the predicted observation density  $p(\boldsymbol{\eta}_{k+1}^* | \mathbf{z}_{1:k}^*)$  for time  $k+1$ , these parameters are transferred to the primary tracking filter and incorporated into the tracking framework. The main objective behind the process of transferring and incorporating the predicted observation parameters is to enhance the accuracy of estimating the state density at time  $k+1$ .

## 4.2 Primary Tracking Filter

Given transferred parameters and observed measurements up to time  $k$ , the posterior density of the state object,  $p(\mathbf{x}_k | \mathbf{z}_{1:k}, \boldsymbol{\eta}_{1:k}^*)$ , can be estimated via the following procedure:

• **Prediction Step:** The mean,  $\hat{\mathbf{x}}_{k|k-1}$ , and covariance matrix,  $\mathbf{P}_{k|k-1}$ , of the predictive density in (20) can be calculated as

$$\begin{aligned} \hat{\mathbf{x}}_{k|k-1} &= E[\mathbf{x}_k | \mathbf{z}_{1:k-1}, \boldsymbol{\eta}_{1:k-1}^*] \\ &= \int_{\mathbb{R}^{n_{\mathbf{x}}}} f_k(\mathbf{x}_{k-1}) p(\mathbf{x}_{k-1} | \mathbf{z}_{1:k-1}, \boldsymbol{\eta}_{1:k-1}^*) d\mathbf{x}_{k-1} \end{aligned} \quad (37)$$

and

$$\begin{aligned} \mathbf{P}_{k|k-1} &= E[(\mathbf{x}_k - \hat{\mathbf{x}}_{k|k-1}) (\mathbf{x}_k - \hat{\mathbf{x}}_{k|k-1})^T | \mathbf{z}_{1:k-1}, \boldsymbol{\eta}_{1:k-1}^*] \\ &= \int_{\mathbb{R}^{n_{\mathbf{x}}}} f_k(\mathbf{x}_{k-1}) (f_k(\mathbf{x}_{k-1}))^T p(\mathbf{x}_{k-1} | \mathbf{z}_{1:k-1}, \boldsymbol{\eta}_{1:k-1}^*) d\mathbf{x}_{k-1} - \hat{\mathbf{x}}_{k|k-1} (\hat{\mathbf{x}}_{k|k-1})^T + \mathbf{Q}_{\mathbf{v},k-1}. \end{aligned} \quad (38)$$

• **Update Step:** In the BTLF framework, the predictive density obtained in the prediction step is updated using two likelihoods, as described in (19). The first likelihood function employed is that of the transferred predicted observation,

which is used to update the density of the object state. This update is performed by leveraging the previously estimated parameters,  $(\hat{\boldsymbol{\eta}}_{k|k-1}^*, \mathbf{P}_{\boldsymbol{\eta}\boldsymbol{\eta},k|k-1}^*)$ , from the source tracking filter at time  $k-1$ . The mean and covariance of the predictive transferred predicted observation density in equation (23) can be computed as follows:

$$\begin{aligned}\hat{\boldsymbol{\eta}}_{k|k-1} &= E[\boldsymbol{\eta}_k | \mathbf{z}_{1:k-1}, \boldsymbol{\eta}_{1:k-1}^*] \\ &= \int_{\mathbb{R}^{n_x}} h_k(\mathbf{x}_k) p(\mathbf{x}_k | \mathbf{z}_{1:k-1}, \boldsymbol{\eta}_{1:k-1}^*) d\mathbf{x}_k\end{aligned}\quad (39)$$

and

$$\begin{aligned}\mathbf{P}_{\boldsymbol{\eta}\boldsymbol{\eta},k|k-1} &= E[(\boldsymbol{\eta}_k - \hat{\boldsymbol{\eta}}_{k|k-1})(\boldsymbol{\eta}_k - \hat{\boldsymbol{\eta}}_{k|k-1})^T | \mathbf{z}_{1:k-1}, \boldsymbol{\eta}_{1:k-1}^*] \\ &= \int_{\mathbb{R}^{n_x}} h_k(\mathbf{x}_k) (h_k(\mathbf{x}_k))^T p(\mathbf{x}_k | \mathbf{z}_{1:k-1}, \boldsymbol{\eta}_{1:k-1}^*) d\mathbf{x}_k - \hat{\boldsymbol{\eta}}_{k|k-1} (\hat{\boldsymbol{\eta}}_{k|k-1})^T + \mathbf{P}_{\boldsymbol{\eta}\boldsymbol{\eta},k|k-1}^*.\end{aligned}\quad (40)$$

The relationship between the state and transferred parameters is characterized by the cross-covariance, expressed as

$$\begin{aligned}\mathbf{P}_{\mathbf{x}\boldsymbol{\eta},k|k-1} &= E[(\mathbf{x}_k - \hat{\mathbf{x}}_{k|k-1})(\boldsymbol{\eta}_k - \hat{\boldsymbol{\eta}}_{k|k-1})^T | \mathbf{z}_{1:k-1}, \boldsymbol{\eta}_{1:k-1}^*] \\ &= \int_{\mathbb{R}^{n_x}} \mathbf{x}_k (h_k(\mathbf{x}_k))^T p(\mathbf{x}_k | \mathbf{z}_{1:k-1}, \boldsymbol{\eta}_{1:k-1}^*) d\mathbf{x}_k \\ &\quad - \hat{\mathbf{x}}_{k|k-1} (\hat{\boldsymbol{\eta}}_{k|k-1})^T.\end{aligned}\quad (41)$$

In the transfer learning framework, the posterior density of the state at time  $k$  given the measurements up to time step  $k-1$  and the transferred parameters up to time  $k$  is assumed to follow a Gaussian distribution, denoted as  $p(\mathbf{x}_k | \mathbf{z}_{1:k-1}, \boldsymbol{\eta}_{2:k}^*) = \mathcal{N}(\mathbf{x}_k; \hat{\mathbf{x}}_{k|k-1}^\eta, \mathbf{P}_{k|k-1}^\eta)$ . The mean and covariance of this state posterior density in the transfer learning framework can be obtained as follows:

$$\hat{\mathbf{x}}_{k|k-1}^\eta = \hat{\mathbf{x}}_{k|k-1} + \mathbf{K}_k^\eta (\hat{\boldsymbol{\eta}}_{k|k-1}^* - \hat{\boldsymbol{\eta}}_{k|k-1})\quad (42)$$

$$\mathbf{P}_{k|k-1}^\eta = \mathbf{P}_{k|k-1} - \mathbf{K}_k^\eta \mathbf{P}_{\boldsymbol{\eta}\boldsymbol{\eta},k|k-1} (\mathbf{K}_k^\eta)^T\quad (43)$$

where the linear gain of the transfer learning framework,  $\mathbf{K}_k^\eta$ , is calculated as

$$\mathbf{K}_k^\eta = \mathbf{P}_{\mathbf{x}\boldsymbol{\eta},k|k-1} (\mathbf{P}_{\boldsymbol{\eta}\boldsymbol{\eta},k|k-1})^{-1}\quad (44)$$

The update process in (42) and (43) integrates the transferred parameters into the tracking framework, refines state density estimation, and incorporates knowledge gained from the source tracking filter. After the state has been updated with the transferred predicted observation likelihood density, the measurement likelihood is incorporated. In this case, the predictive measurement density  $p(\mathbf{z}_k | \mathbf{z}_{1:k-1}, \boldsymbol{\eta}_{1:k}^*)$  in equation (24) is assumed to be a Gaussian distribution with mean and covariance can be computed as

$$\begin{aligned}\hat{\mathbf{z}}_{k|k-1} &= E[\mathbf{z}_k | \mathbf{z}_{1:k-1}, \boldsymbol{\eta}_{1:k}^*] \\ &= \int_{\mathbb{R}^{n_x}} h_k(\mathbf{x}_k) p(\mathbf{x}_k | \mathbf{z}_{1:k-1}, \boldsymbol{\eta}_{1:k}^*) d\mathbf{x}_k\end{aligned}\quad (45)$$

and

$$\begin{aligned}\mathbf{P}_{\mathbf{z}\mathbf{z},k|k-1} &= E[(\mathbf{z}_k - \hat{\mathbf{z}}_{k|k-1})(\mathbf{z}_k - \hat{\mathbf{z}}_{k|k-1})^T | \mathbf{z}_{1:k-1}, \boldsymbol{\eta}_{1:k}^*] \\ &= \int_{\mathbb{R}^{n_x}} h_k(\mathbf{x}_k) (h_k(\mathbf{x}_k))^T p(\mathbf{x}_k | \mathbf{z}_{1:k-1}, \boldsymbol{\eta}_{1:k}^*) d\mathbf{x}_k - \hat{\mathbf{z}}_{k|k-1} (\hat{\mathbf{z}}_{k|k-1})^T + \mathbf{Q}_{\mathbf{w},k}.\end{aligned}\quad (46)$$

The cross-covariance between the state and the measurement determines the relationship and dependence of the state and the measurement, defined as

$$\begin{aligned}\mathbf{P}_{\mathbf{x}\mathbf{z},k|k-1} &= E[(\mathbf{x}_k - \hat{\mathbf{x}}_{k|k-1})(\mathbf{z}_k - \hat{\mathbf{z}}_{k|k-1})^T | \mathbf{z}_{1:k-1}, \boldsymbol{\eta}_{1:k}^*] \\ &= \int_{\mathbb{R}^{n_x}} \mathbf{x}_k (h_k(\mathbf{x}_k))^T p(\mathbf{x}_k | \mathbf{z}_{1:k-1}, \boldsymbol{\eta}_{1:k}^*) d\mathbf{x}_k - \hat{\mathbf{x}}_{k|k-1}^\eta (\hat{\mathbf{z}}_{k|k-1})^T.\end{aligned}\quad (47)$$



The posterior density of the overall state in (19) can be estimated based on the newly acquired observed measurement. This density is modeled as a Gaussian distribution, described as  $p(\mathbf{x}_k | \mathbf{z}_{1:k}, \boldsymbol{\eta}_{2:k}^*) = \mathcal{N}(\mathbf{x}_k; \hat{\mathbf{x}}_{k|k}, \mathbf{P}_{k|k})$ . The mean and covariance of this overall density can be estimated as follows:

$$\hat{\mathbf{x}}_{k|k} = \hat{\mathbf{x}}_{k|k-1}^\eta + \mathbf{K}_k (\mathbf{z}_k - \hat{\mathbf{z}}_{k|k-1}), \quad (48)$$

$$\mathbf{P}_{k|k} = \mathbf{P}_{k|k-1}^\eta - \mathbf{K}_k \mathbf{P}_{\mathbf{z}\mathbf{z},k|k-1} (\mathbf{K}_k)^T, \quad (49)$$

where the gain,  $\mathbf{K}_k$ , is defined as

$$\mathbf{K}_k = \mathbf{P}_{\mathbf{x}\mathbf{z},k|k-1} (\mathbf{P}_{\mathbf{z}\mathbf{z},k|k-1})^{-1}. \quad (50)$$

After estimating the mean and covariance via (48) and (49), the overall posterior density of the state is estimated by leveraging transferred knowledge from the source tracking filter. Incorporating BTLF approach by utilizing and leveraging transferred knowledge improves the accuracy of the estimation process, yielding more reliable and accurate estimation of the state.

## 5 Transfer Learning for UKF

The UKF [3] uses a set of sigma points to approximate a nonlinear function, unlike the extended Kalman filter (EKF) which relies on linearization. In situations where analytical Jacobians of the transition and measurement model functions are unavailable, this feature provides the UKF an significant advantage over the EKF [23]. Due to its advantages over the EKF, the UKF is chosen as a local approach to approximate the BTLF, described Section 3, where knowledge is transferred from the source to the primary tracking filter and used as a prior to improve the accuracy of object state estimation.

### 5.1 Source Tracking Filter

By applying the UT method [3], the set of  $2n_{\mathbf{x}} + 1$  sigma points are defined as

$$\boldsymbol{\chi}_{0,k-1|k-1}^* = \hat{\mathbf{x}}_{k-1|k-1}^* \quad (51)$$

$$\boldsymbol{\chi}_{j,k-1|k-1}^* = \hat{\mathbf{x}}_{k-1|k-1}^* + \sqrt{(n_{\mathbf{x}} + \lambda) \mathbf{P}_{j,k-1|k-1}^*} \quad (52)$$

$$\boldsymbol{\chi}_{n_{\mathbf{x}}+j,k-1|k-1}^* = \hat{\mathbf{x}}_{k-1|k-1}^* - \sqrt{(n_{\mathbf{x}} + \lambda) \mathbf{P}_{j,k-1|k-1}^*}, \quad (53)$$

where  $j = 1, \dots, n_{\mathbf{x}}$  and  $\lambda = \alpha^2 (n_{\mathbf{x}} + \kappa) - n_{\mathbf{x}}$  is a scaling parameter consisting of  $10^{-4} \leq \alpha \leq 1$ . The value of  $\kappa$  is defined by  $\kappa = 3 - n_{\mathbf{x}}$ , as suggested in [3]. Furthermore,  $\mathbf{P}_{j,k-1|k-1}^*$  refers to the  $j$ th column of the covariance matrix. The associated weights of these sigma points are obtained as

$$W_{0,k}^* = \frac{\lambda}{n_{\mathbf{x}} + \lambda}, \quad W_{j,k}^* = \frac{1}{2n_{\mathbf{x}} + 2\lambda}, \quad (54)$$

for  $j = 1, 2, \dots, 2n_{\mathbf{x}}$ .

• **Prediction Step:** The mean  $\hat{\mathbf{x}}_{k|k-1}^*$  and the associated covariance  $\mathbf{P}_{k|k-1}^*$  for the predictive density can be estimated as

$$\hat{\mathbf{x}}_{k|k-1}^* = \sum_{j=0}^{2n_{\mathbf{x}}} W_{j,k}^* f(\boldsymbol{\chi}_{j,k-1|k-1}^*), \quad (55)$$

$$\mathbf{P}_{k|k-1}^* = \sum_{j=0}^{2n_{\mathbf{x}}} W_{j,k}^* \left[ f(\boldsymbol{\chi}_{j,k-1|k-1}^*) - \hat{\mathbf{x}}_{k|k-1}^* \right] \left[ f(\boldsymbol{\chi}_{j,k-1|k-1}^*) - \hat{\mathbf{x}}_{k|k-1}^* \right]^T + \mathbf{Q}_{\mathbf{v}}^*. \quad (56)$$

By applying the nonlinear transition model function to the sigma points, the predicted sigma points  $\boldsymbol{\chi}_{j,k|k-1}^*$  can be obtained as

$$\boldsymbol{\chi}_{j,k|k-1}^* = f(\boldsymbol{\chi}_{j,k-1|k-1}^*). \quad (57)$$

• **Update Step:** The predicted measurement mean  $\hat{\mathbf{z}}_{k|k-1}^*$  and the associated covariance  $\mathbf{P}_{\mathbf{zz},k|k-1}^*$  can be computed as

$$\hat{\mathbf{z}}_{k|k-1}^* = \sum_{j=0}^{2n_x} W_{j,k}^* h(\mathbf{x}_{j,k|k-1}^*) \quad (58)$$

$$\mathbf{P}_{\mathbf{zz},k|k-1}^* = \sum_{j=0}^{2n_x} W_{j,k}^* \left[ h(\mathbf{x}_{j,k|k-1}^*) - \hat{\mathbf{z}}_{k|k-1}^* \right] \left[ h(\mathbf{x}_{j,k|k-1}^*) - \hat{\mathbf{z}}_{k|k-1}^* \right]^T + \mathbf{Q}_w^*. \quad (59)$$

The joint conditional density's cross-covariance can be computed as follows:

$$\mathbf{P}_{\mathbf{xz},k|k-1}^* = \sum_{j=0}^{2n_x} W_{j,k}^* \left[ f(\mathbf{x}_{j,k-1|k-1}^*) - \hat{\mathbf{x}}_{k|k-1}^* \right] \left[ h(\mathbf{x}_{j,k|k-1}^*) - \hat{\mathbf{z}}_{k|k-1}^* \right]^T. \quad (60)$$

After observing the new measurement, the posterior density of the object state can be estimated with the mean  $\hat{\mathbf{x}}_{k|k}^*$  and covariance  $\mathbf{P}_{k|k}^*$ , computed as follows:

$$\hat{\mathbf{x}}_{k|k}^* = \hat{\mathbf{x}}_{k|k-1}^* + \mathbf{K}_k^* (\mathbf{z}_k^* - \hat{\mathbf{z}}_{k|k-1}^*), \quad (61)$$

$$\mathbf{P}_{k|k}^* = \mathbf{P}_{k|k-1}^* - \mathbf{K}_k^* \mathbf{P}_{\mathbf{zz},k|k-1}^* (\mathbf{K}_k^*)^T, \quad (62)$$

where the Kalman gain  $\mathbf{K}_k^*$  is computed as

$$\mathbf{K}_k^* = \mathbf{P}_{\mathbf{xz},k|k-1}^* (\mathbf{P}_{\mathbf{zz},k|k-1}^*)^{-1}. \quad (63)$$

• **Predict Observation Step:** The predicted observation variable set  $\boldsymbol{\eta}^*$  is introduced in the BTLEF via the posterior density of the predicted observation  $p(\boldsymbol{\eta}_{k+1}^* | \mathbf{z}_{1:k}^*)$  in (11), where  $\boldsymbol{\eta}_{k+1}^* \sim \mathcal{N}(\hat{\boldsymbol{\eta}}_{k+1|k}^*, \mathbf{P}_{\boldsymbol{\eta}\boldsymbol{\eta},k+1|k}^*)$  is a Gaussian vector with mean  $\hat{\boldsymbol{\eta}}_{k+1|k}^*$  and associated covariance  $\mathbf{P}_{\boldsymbol{\eta}\boldsymbol{\eta},k+1|k}^*$  computed by following the procedures as:

$$\boldsymbol{\mathcal{X}}_{0,k|k}^* = \hat{\mathbf{x}}_{k|k}^* \quad (64)$$

$$\boldsymbol{\mathcal{X}}_{j,k|k}^* = \hat{\mathbf{x}}_{k|k}^* + \sqrt{(n_x + \lambda) \mathbf{P}_{j,k|k}^*} \quad (65)$$

$$\boldsymbol{\mathcal{X}}_{n_x+j,k|k}^* = \hat{\mathbf{x}}_{k|k}^* - \sqrt{(n_x + \lambda) \mathbf{P}_{j,k|k}^*} \quad (66)$$

$$\boldsymbol{\mathcal{X}}_{j,k+1|k}^* = f(\boldsymbol{\mathcal{X}}_{j,k|k}^*) \quad (67)$$

$$\hat{\boldsymbol{\eta}}_{k+1|k}^* = \sum_{j=0}^{2n_x} W_{j,k}^* h(\boldsymbol{\mathcal{X}}_{j,k+1|k}^*), \quad (68)$$

where  $j = 1, 2, \dots, n_x$  and

$$\mathbf{P}_{\boldsymbol{\eta}\boldsymbol{\eta},k+1|k}^* = \sum_{j=0}^{2n_x} W_{j,k}^* \left[ h(\boldsymbol{\mathcal{X}}_{j,k+1|k}^*) - \hat{\boldsymbol{\eta}}_{k+1|k}^* \right] \left[ h(\boldsymbol{\mathcal{X}}_{j,k+1|k}^*) - \hat{\boldsymbol{\eta}}_{k+1|k}^* \right]^T + \mathbf{Q}_w^*. \quad (69)$$

The posterior density of the predicted observation  $p(\boldsymbol{\eta}_{k+1}^* | \mathbf{z}_{1:k}^*)$  follows a Gaussian distribution with the mean and covariance estimated in (68) and (69), respectively. The predicted observation parameters  $\hat{\boldsymbol{\eta}}_{k+1|k}^*$  and  $\mathbf{P}_{\boldsymbol{\eta}\boldsymbol{\eta},k+1|k}^*$  are transferred to the primary tracking filter and utilized as a prior to improve estimation accuracy.

## 5.2 Primary Tracking Filter

Equivalently to the source tracking filter, the set of  $2n_x + 1$  sigma points and their associated weights in the primary tracking filter can be drawn and computed as follows:

$$\boldsymbol{\mathcal{X}}_{0,k-1|k-1} = \hat{\mathbf{x}}_{k-1|k-1}, \quad (70)$$

$$\boldsymbol{\mathcal{X}}_{j,k-1|k-1} = \hat{\mathbf{x}}_{k-1|k-1} + \sqrt{(n_x + \lambda) \mathbf{P}_{j,k-1|k-1}}, \quad (71)$$

$$\boldsymbol{\mathcal{X}}_{n_x+j,k-1|k-1} = \hat{\mathbf{x}}_{k-1|k-1} - \sqrt{(n_x + \lambda) \mathbf{P}_{j,k-1|k-1}}, \quad (72)$$

$$W_{0,k} = \frac{\lambda}{n_{\mathbf{x}} + \lambda}, \quad W_{j,k} = \frac{1}{2n_{\mathbf{x}} + 2\lambda}, \quad (73)$$

where  $j = 1, 2, \dots, n_{\mathbf{x}}$ .

• **Prediction Step:** The predictive density mean  $\hat{\mathbf{x}}_{k|k-1}$  and covariance  $\mathbf{P}_{k|k-1}$  can be estimated as follows:

$$\hat{\mathbf{x}}_{k|k-1} = \sum_{j=0}^{2n_{\mathbf{x}}} W_{j,k} f(\mathbf{x}_{j,k-1|k-1}) \quad (74)$$

$$\mathbf{P}_{k|k-1} = \sum_{j=0}^{2n_{\mathbf{x}}} W_{j,k} \left[ f(\mathbf{x}_{j,k-1|k-1}) - \hat{\mathbf{x}}_{k|k-1} \right] \left[ f(\mathbf{x}_{j,k-1|k-1}) - \hat{\mathbf{x}}_{k|k-1} \right]^T + \mathbf{Q}_{\mathbf{v}}. \quad (75)$$

The drawn sigma points in (70) are advanced one time step using the nonlinear transition function as follows:

$$\mathbf{x}_{j,k|k-1} = f(\mathbf{x}_{j,k-1|k-1}). \quad (76)$$

• **Update Step:** The predicted object state density in the primary tracking filter is updated using two likelihood functions by incorporating transfer learning, as represented in (19), into the UKF framework. In the initial stage, the transferred predicted observation likelihood function  $p(\boldsymbol{\eta}_k^* | \mathbf{x}_k)$  is employed to update the predicted object state density. This update process incorporates the transferred parameters,  $\hat{\boldsymbol{\eta}}_{k|k-1}^*$  and  $\mathbf{P}_{\boldsymbol{\eta}\boldsymbol{\eta},k|k-1}^*$ , which were estimated in the previous time step  $k-1$  in the source filter, into the process. The predicted mean  $\hat{\boldsymbol{\eta}}_{k|k-1}$  and covariance  $\mathbf{P}_{\boldsymbol{\eta}\boldsymbol{\eta},k|k-1}$  for the transferred predicted observation can be computed as

$$\hat{\boldsymbol{\eta}}_{k|k-1} = \sum_{j=0}^{2n_{\mathbf{x}}} W_{j,k} h(\mathbf{x}_{j,k|k-1}), \quad (77)$$

$$\mathbf{P}_{\boldsymbol{\eta}\boldsymbol{\eta},k|k-1} = \sum_{j=0}^{2n_{\mathbf{x}}} W_{j,k} \left[ h(\mathbf{x}_{j,k|k-1}) - \hat{\boldsymbol{\eta}}_{k|k-1} \right] \left[ h(\mathbf{x}_{j,k|k-1}) - \hat{\boldsymbol{\eta}}_{k|k-1} \right]^T + \mathbf{P}_{\boldsymbol{\eta}\boldsymbol{\eta},k|k-1}^*. \quad (78)$$

The cross-covariance, which characterizes the relationship between the state and the transferred parameter, is defined as

$$\mathbf{P}_{\mathbf{x}\boldsymbol{\eta},k|k-1} = \sum_{j=0}^{2n_{\mathbf{x}}} W_{j,k} \left[ f(\mathbf{x}_{j,k-1|k-1}) - \hat{\mathbf{x}}_{k|k-1} \right] \left[ h(\mathbf{x}_{j,k|k-1}) - \hat{\boldsymbol{\eta}}_{k|k-1} \right]^T. \quad (79)$$

Given the transferred parameter  $\boldsymbol{\eta}_k^*$ , the posterior density of the state in the transfer learning framework, denoted as  $p(\mathbf{x}_k | \mathbf{z}_{1:k-1}, \boldsymbol{\eta}_{2:k}^*) \sim \mathcal{N}(\mathbf{x}_k; \hat{\mathbf{x}}_{k|k-1}^{\boldsymbol{\eta}}, \mathbf{P}_{k|k-1}^{\boldsymbol{\eta}})$ , is estimated with mean  $\hat{\mathbf{x}}_{k|k-1}^{\boldsymbol{\eta}}$  and covariance  $\mathbf{P}_{k|k-1}^{\boldsymbol{\eta}}$  as

$$\hat{\mathbf{x}}_{k|k-1}^{\boldsymbol{\eta}} = \hat{\mathbf{x}}_{k|k-1} + \mathbf{K}_k^{\boldsymbol{\eta}} (\hat{\boldsymbol{\eta}}_{k|k-1}^* - \hat{\boldsymbol{\eta}}_{k|k-1}), \quad (80)$$

$$\mathbf{P}_{k|k-1}^{\boldsymbol{\eta}} = \mathbf{P}_{k|k-1} - \mathbf{K}_k^{\boldsymbol{\eta}} \mathbf{P}_{\boldsymbol{\eta}\boldsymbol{\eta},k|k-1} (\mathbf{K}_k^{\boldsymbol{\eta}})^T, \quad (81)$$

where the Kalman gain of the transfer learning framework  $\mathbf{K}_k^{\boldsymbol{\eta}}$  is given by

$$\mathbf{K}_k^{\boldsymbol{\eta}} = \mathbf{P}_{\mathbf{x}\boldsymbol{\eta},k|k-1} (\mathbf{P}_{\boldsymbol{\eta}\boldsymbol{\eta},k|k-1})^{-1}. \quad (82)$$

Based on the estimated mean and covariance of the transfer learning state posterior density computed in (80) and (81) respectively, the set of  $2n_{\mathbf{x}} + 1$  sigma points will be redrawn as

$$\mathbf{x}_{0,k|k-1}^{\boldsymbol{\eta}} = \hat{\mathbf{x}}_{k|k-1}^{\boldsymbol{\eta}}, \quad (83)$$

$$\mathbf{x}_{j,k|k-1}^{\boldsymbol{\eta}} = \hat{\mathbf{x}}_{k|k-1}^{\boldsymbol{\eta}} + \sqrt{(n_{\mathbf{x}} + \lambda) \mathbf{P}_{j,k|k-1}^{\boldsymbol{\eta}}}, \quad (84)$$

$$\mathbf{x}_{n_{\mathbf{x}}+j,k|k-1}^{\boldsymbol{\eta}} = \hat{\mathbf{x}}_{k|k-1}^{\boldsymbol{\eta}} - \sqrt{(n_{\mathbf{x}} + \lambda) \mathbf{P}_{j,k|k-1}^{\boldsymbol{\eta}}}, \quad (85)$$

where  $j = 1, 2, \dots, n_{\mathbf{x}}$ . The estimated measurement mean and covariance can be calculated as follows:

$$\hat{\mathbf{z}}_{k|k-1} = \sum_{j=0}^{2n_{\mathbf{x}}} W_{j,k} h\left(\boldsymbol{\chi}_{j,k|k-1}^{\eta}\right), \quad (86)$$

$$\mathbf{P}_{\mathbf{zz},k|k-1} = \sum_{j=0}^{2n_{\mathbf{x}}} W_{j,k} \left[ h\left(\boldsymbol{\chi}_{j,k|k-1}^{\eta}\right) - \hat{\mathbf{z}}_{k|k-1} \right] \left[ h\left(\boldsymbol{\chi}_{j,k|k-1}^{\eta}\right) - \hat{\mathbf{z}}_{k|k-1} \right]^T + \mathbf{Q}_{\mathbf{w}}. \quad (87)$$

The cross-covariance matrix, which expresses the relationship between state and measurement in the joint density, is computed as follows:

$$\mathbf{P}_{\mathbf{xz},k|k-1} = \sum_{j=0}^{2n_{\mathbf{x}}} W_{j,k} \left[ \boldsymbol{\chi}_{j,k|k-1}^{\eta} - \hat{\mathbf{x}}_{k|k-1}^{\eta} \right] \left[ h\left(\boldsymbol{\chi}_{j,k|k-1}^{\eta}\right) - \hat{\mathbf{z}}_{k|k-1} \right]^T. \quad (88)$$

Similarly to the source tracking filter, upon observing the measurement  $\mathbf{z}_k$ , the estimated mean and covariance of the posterior density are computed as

$$\hat{\mathbf{x}}_{k|k} = \hat{\mathbf{x}}_{k|k-1}^{\eta} + \mathbf{K}_k (\mathbf{z}_k - \hat{\mathbf{z}}_{k|k-1}), \quad (89)$$

$$\mathbf{P}_{k|k} = \mathbf{P}_{k|k-1}^{\eta} - \mathbf{K}_k \mathbf{P}_{\mathbf{zz},k|k-1} (\mathbf{K}_k)^T, \quad (90)$$

where  $\mathbf{K}_k$  denotes the Kalman gain defined by

$$\mathbf{K}_k = \mathbf{P}_{\mathbf{xz},k|k-1} (\mathbf{P}_{\mathbf{zz},k|k-1})^{-1}. \quad (91)$$

The posterior density of the state, conditioned on the observed measurement and the transferred predicted observation parameters, denoted as  $p(\mathbf{x}_k | \mathbf{z}_{1:k}, \boldsymbol{\eta}_{2:k}^*) = \mathcal{N}(\mathbf{x}_k; \hat{\mathbf{x}}_{k|k}, \mathbf{P}_{k|k})$ , given in (19), is modeled as a Gaussian density. The mean and covariance of this posterior density are estimated via (89) and (90), respectively.

Appendix A provides an outline of the algorithms for UKF with transfer learning in both the source and primary tracking filters. These algorithms include the specific steps and procedures for implementing the proposed approach.

## 6 Numerical Instability in the UKF

The UKF employs the UT to approximate the underlying distribution using sigma points. These sigma points are strategically drawn to approximate a standard Gaussian distribution with a dimension of  $n_{\mathbf{x}}$ . The process of drawing these sigma points through the UT involves a scaling parameter  $\kappa$ , which introduces additional flexibility for scaling higher-order moments. It is important to note that  $\kappa$  can be either positive or negative, but it must satisfy the condition  $n_{\mathbf{x}} + \kappa \neq 0$ .

The moments of the sigma points differ from those of a standard Gaussian distribution. To minimize the impact of these differences and reduce the approximation errors, it is suggested to set  $n_{\mathbf{x}} + \kappa = 3$ . This choice ensures that the moments of the sigma points align with the moments of a standard Gaussian distribution up to the fourth order. When moments are matched up to the fourth order for Gaussian cases, the accuracy of the approximation process is improved [24].

In scenarios where the system dimension  $n_{\mathbf{x}} > 3$ , the suggested value of  $\kappa$  in [3], i.e.,  $\kappa = 3 - n_{\mathbf{x}}$ , results in a negative value for  $\kappa$ . This introduces challenges to the UKF algorithm. First, the central sigma point  $\boldsymbol{\chi}_0$ , which represents the mean, will have a negative weight  $W_0 < 0$ . This means that the central point, which is typically considered more important and carries a higher weight, is assigned a negative weight. Second, estimating the covariance matrix can become problematic as it may lose positive semi-definiteness [3]. This loss of positive semi-definiteness can result in numerical instability of the UKF algorithm [4]. These considerations highlight the need to address the implications of negative  $\kappa$  values on the stability and accuracy of the UKF algorithm in high-dimensional systems.

To address the stability of an integration rule, the absolute values of the integration rule weights must be summed to unity. This condition ensures that the integration rule is completely stable [25]. Applying this stability measure to the weights of the UKF algorithm identifies numerical instability issues that pose challenges to the algorithm. The stability factor can be computed as

$$\begin{aligned} \sum_{j=0}^{2n_{\mathbf{x}}} |W_j| &= \left| \frac{\lambda}{n_{\mathbf{x}} + \lambda} \right| + \left| \frac{1}{2n_{\mathbf{x}} + 2\lambda} \right| + \dots + \left| \frac{1}{2n_{\mathbf{x}} + 2\lambda} \right| \\ &= \left| \frac{\lambda}{n_{\mathbf{x}} + \lambda} \right| + 2n_{\mathbf{x}} \left| \frac{1}{2n_{\mathbf{x}} + 2\lambda} \right| = \frac{n_{\mathbf{x}} + |\lambda|}{|n_{\mathbf{x}} + \lambda|}, \end{aligned} \quad (92)$$

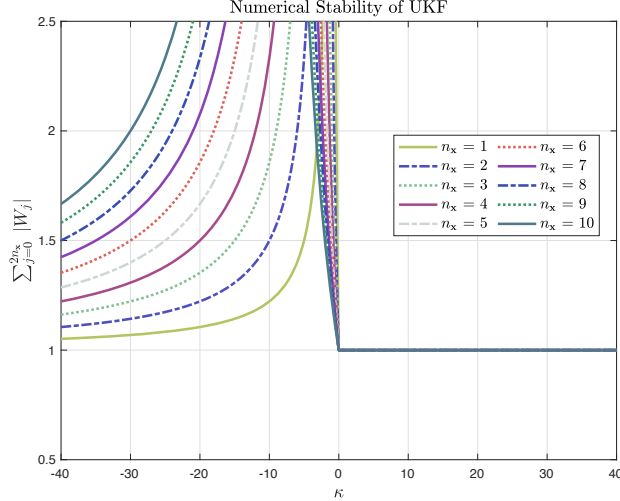


Figure 3: The stability measure addresses the impact of the  $\kappa$  value on the stability of the UKF across various dimensions,  $n_x$ .

where  $\sum_{j=0}^{2n_x} |W_j|$  should be unity to ensure the stability of the UKF algorithm. Therefore, we must have  $n_x + |\lambda| = |n_x + \lambda|$ . To simplify the analysis, we assume  $\alpha = 1$ , which implies that  $\lambda = \kappa$ . Then the stability condition for the UKF, can be expressed as  $n_x + |\kappa| = |n_x + \kappa|$ . In Fig. 3, the influence of different values of  $\kappa$  on the stability measure factor in different dimensions is examined. This demonstrates that the stability condition holds true only when  $\kappa \geq 0$ , indicating that the UKF is stable when  $\kappa$  is nonnegative.

The value of  $\kappa$  plays a crucial role in the numerical stability and estimation accuracy of the UKF. Within the transfer learning framework of UKF, the predict observation step in the source tracking filter, as described from (64) to (69), can be influenced by the value of  $\kappa$ . A negative value of  $\kappa$  can lead to inaccurate estimation of the predicted observation density parameters,  $(\hat{\eta}^*, \mathbf{P}_{\eta\eta}^*)$ , which in turn results in inaccurate parameter estimates being transferred to the primary tracking filter and consequently, poor estimation accuracy at the primary sensor. To mitigate numerical instability issues, the value of  $\kappa$  can be set to zero or a positive value for high-dimensional systems ( $n_x > 3$ ). Setting  $\kappa$  to zero is a common solution, which effectively cancels out the central sigma point. However, the UKF with  $\kappa = 0$  is identical to the third-degree CKF. Therefore, the third-degree CKF can be considered as a special case of the UKF [26, 27].

## 7 Transfer Learning for CKF

The cubature rule has been introduced by as a non-product rule to solve weighted integrals that are difficult to compute, specifically Gaussian weighted integrals [4]. The cubature rule approximates these Gaussian integrals using a set of points with associated weights, similar to the UT approximation. As mentioned in the previous section, the third-degree CKF is considered a special case of the UKF with  $\kappa = 0$  and was introduced as a solution for the numerical instability issue that faces the UKF when  $\kappa < 0$ , in the case of high dimensional system. To improve the estimation accuracy of the third-degree CKF is limited, a fifth-degree CKF was proposed in [26]. In this section, the third-degree and fifth-degree CKFs are integrated into the BTLF. The objective is to improve the estimation accuracy of both CKFs by integrating transfer learning for sharing knowledge from the source to the primary tracking filter.

### 7.1 Transfer Learning for Third-degree CKF

The implementation of the third-degree CKF follows a similar approach to that of the UKF to approximate BTLF. However, the CKF differs from the UKF in the manner in which the set of weighted points is drawn. Instead of using the UT, the CKF employs the cubature rule method. Specifically, the third-degree CKF uses the following set of  $2n_x$

sigma points:

$$\mathcal{X}_{j,k-1|k-1} = \hat{\mathbf{x}}_{k-1|k-1} + \sqrt{n_{\mathbf{x}} \mathbf{P}_{j,k-1|k-1}} \quad (93)$$

$$\mathcal{X}_{n_{\mathbf{x}}+j,k-1|k-1} = \hat{\mathbf{x}}_{k-1|k-1} - \sqrt{n_{\mathbf{x}} \mathbf{P}_{j,k-1|k-1}}, \quad (94)$$

where  $j = 1, \dots, n_{\mathbf{x}}$ , and the associated weights of these sigma points assigned as:

$$W_{j,k} = \frac{1}{2n_{\mathbf{x}}}, \quad j = 1, \dots, n_{\mathbf{x}}. \quad (95)$$

The sigma points used in the third-degree CKF can be utilized to approximate the BTLF effectively in the source and primary tracking systems for estimating posterior densities. It is noteworthy that the associated weights for each sigma point, as indicated in (95) depend only on the dimension  $n_{\mathbf{x}}$ . This guarantees that the weights associated with the sigma points are strictly positive, thus improving the numerical stability of the third-degree CKF relative to a UKF with a negative value of  $\kappa$  (see Section 6). Conversely, the central sigma point, which represents the mean in the UKF, is eliminated in (93). Furthermore, the distance between these chosen sigma points and the mean is proportional to the dimension  $n_{\mathbf{x}}$ , which introduces a non-local sampling issue [27, 28].

## 7.2 Transfer Learning for Fifth-degree CKF

Equivalent to the third-degree CKF, the fifth-degree of the CKF is based on the spherical-radial cubature rule. However, it extends the degree of accuracy to the fifth degree by utilizing a set of weighted points consisting of  $2n_{\mathbf{x}}^2 + 1$  sigma points to compute Gaussian weighted integrals, drawn as follows:

$$\begin{aligned} \mathcal{X}_{0,k-1|k-1} &= \hat{\mathbf{x}}_{k-1|k-1} \\ \mathcal{X}_{j_a,k-1|k-1} &= \hat{\mathbf{x}}_{k-1|k-1} + \gamma \sqrt{\mathbf{P}_{j_a,k-1|k-1}} \\ \mathcal{X}_{n_{\mathbf{x}}+j_a,k-1|k-1} &= \hat{\mathbf{x}}_{k-1|k-1} - \gamma \sqrt{\mathbf{P}_{j_a,k-1|k-1}} \\ \mathcal{X}_{2n_{\mathbf{x}}+j_b,k-1|k-1} &= \hat{\mathbf{x}}_{k-1|k-1} + \gamma \sqrt{\mathbf{P}_{j_b,k-1|k-1}^+} \\ \mathcal{X}_{\frac{n_{\mathbf{x}}(n_{\mathbf{x}}+3)}{2}+j_b,k-1|k-1} &= \hat{\mathbf{x}}_{k-1|k-1} - \gamma \sqrt{\mathbf{P}_{j_b,k-1|k-1}^+} \\ \mathcal{X}_{n_{\mathbf{x}}(n_{\mathbf{x}}+1)+j_b,k-1|k-1} &= \hat{\mathbf{x}}_{k-1|k-1} + \gamma \sqrt{\mathbf{P}_{j_b,k-1|k-1}^-} \\ \mathcal{X}_{\frac{n_{\mathbf{x}}(3n_{\mathbf{x}}+1)}{2}+j_b,k-1|k-1} &= \hat{\mathbf{x}}_{k-1|k-1} - \gamma \sqrt{\mathbf{P}_{j_b,k-1|k-1}^-}, \end{aligned} \quad (96)$$

where  $j_a = 1, \dots, n_{\mathbf{x}}$ ,  $j_b = 1, \dots, \frac{n_{\mathbf{x}}(n_{\mathbf{x}}-1)}{2}$ , and  $\gamma = \sqrt{(n_{\mathbf{x}} + 2)}$ . The matrices  $\mathbf{P}_{j_b,k-1|k-1}^+$  and  $\mathbf{P}_{j_b,k-1|k-1}^-$  in (96) are defined, respectively, as

$$\sqrt{\mathbf{P}_{j_b,k-1|k-1}^+} = 2^{-\frac{1}{2}} \left[ \sqrt{\mathbf{P}_{a,k-1|k-1}} + \sqrt{\mathbf{P}_{b,k-1|k-1}} \right], \quad (97)$$

where  $a < b$ ,  $a, b = 1, \dots, n_{\mathbf{x}}$  and

$$\sqrt{\mathbf{P}_{j_b,k-1|k-1}^-} = 2^{-\frac{1}{2}} \left[ \sqrt{\mathbf{P}_{a,k-1|k-1}} - \sqrt{\mathbf{P}_{b,k-1|k-1}} \right], \quad (98)$$

where  $a < b$ ,  $a, b = 1, \dots, n_{\mathbf{x}}$ . The set of  $2n_{\mathbf{x}}^2 + 1$  sigma points are weighted as follows:

$$W_{j,k} = \begin{cases} \frac{2}{n_{\mathbf{x}}+2}, & j = 0, \\ \frac{4-n_{\mathbf{x}}}{2(n_{\mathbf{x}}+2)^2}, & j = 1, \dots, 2n_{\mathbf{x}}, \\ \frac{1}{(n_{\mathbf{x}}+2)^2}, & j = 2n_{\mathbf{x}} + 1, \dots, 2n_{\mathbf{x}}^2. \end{cases} \quad (99)$$

As indicated in (99), the weights associated with the fifth-degree CKF can be negative, potentially leading to numerical instability. To address this concern, the stability measure can be applied to the weights of the fifth-degree CKF. The resulting summation of the absolute values of the weights is given by

$$\sum_{j=0}^{2n_{\mathbf{x}}^2} |W_j| = \frac{n_{\mathbf{x}} |4 - n_{\mathbf{x}}| + 2n_{\mathbf{x}}^2 + 4}{(n_{\mathbf{x}} + 2)^2}. \quad (100)$$

According to the stability measure factor derived in (100), the fifth-degree CKF achieves complete stability only when the dimension satisfies  $n_x \leq 4$ . However, in the case of high-dimensional systems where  $n_x > 4$ , the stability of the fifth-degree CKF is less than that of the third-degree CKF. Nevertheless, it is worth emphasizing that the central sigma point  $\mathcal{X}_0$  of the fifth-degree CKF will still carry a positive weight even for high-dimensional systems, which provides an advantage over the UKF with a negative value of  $\kappa$ , where its central sigma point has a negative weight.

## 8 Simulation Results

We consider the problem of estimating the unknown state vector  $\mathbf{x}_k = [x_k, \dot{x}_k, y_k, \dot{y}_k, \Omega_k]^T$  associated with a single object undergoing constant velocity motion in a two-dimensional trajectory. The state vector comprises the Cartesian coordinates  $(x_k, y_k)$ , the object's velocity  $(\dot{x}_k, \dot{y}_k)$ , and the turn rate  $\Omega_k$ . Our approach adopts a state transition model based on a nonlinear process model employed in [29], which is given by

$$\mathbf{x}_k = \begin{bmatrix} 1 & \frac{\sin(\Omega_{k-1}T_s)}{\Omega_{k-1}} & 0 & -\left(\frac{1-\cos(\Omega_{k-1}T_s)}{\Omega_{k-1}}\right) & 0 \\ 0 & \cos(\Omega_{k-1}T_s) & 0 & -\sin(\Omega_{k-1}T_s) & 0 \\ 0 & \frac{1-\cos(\Omega_{k-1}T_s)}{\Omega_{k-1}} & 1 & \frac{\sin(\Omega_{k-1}T_s)}{\Omega_{k-1}} & 0 \\ 0 & \sin(\Omega_{k-1}T_s) & 0 & \cos(\Omega_{k-1}T_s) & 0 \\ 0 & 0 & 0 & 0 & 1 \end{bmatrix} \mathbf{x}_{k-1} + \mathbf{v}_{k-1}, \quad (101)$$

where the process noise  $\mathbf{v}_{k-1} \sim \mathcal{N}(0, \mathbf{Q}_v)$  with

$$\mathbf{Q}_v = \begin{bmatrix} q_1 \frac{T_s^4}{4} & q_1 \frac{T_s^3}{2} & 0 & 0 & 0 \\ q_1 \frac{T_s^3}{2} & q_1 T_s^2 & 0 & 0 & 0 \\ 0 & 0 & q_1 \frac{T_s^4}{4} & q_1 \frac{T_s^3}{2} & 0 \\ 0 & 0 & q_1 \frac{T_s^3}{2} & q_1 T_s^2 & 0 \\ 0 & 0 & 0 & 0 & q_2 T_s \end{bmatrix}. \quad (102)$$

In order to ensure a fair comparison, we make the assumption that both the source and primary filters possess identical error process noise covariances, i.e.,  $\mathbf{Q}_v^* = \mathbf{Q}_v$ .

### 8.1 Parameters Settings

The measurement vector at time  $k$ , denoted by  $\mathbf{z}_k$ , consists of the object's range  $r_k$  and angle  $\zeta_k$ . The measurements obtained from the sensors in both the source and primary tracking filters are affected by Gaussian noise, which are modeled by the following equations:

$$\mathbf{z}_k^* = h(\mathbf{x}_k) + \mathbf{w}_k^*, \quad \mathbf{w}_k^* \sim \mathcal{N}(0, \mathbf{Q}_w^*), \quad (103)$$

$$\mathbf{z}_k = h(\mathbf{x}_k) + \mathbf{w}_k, \quad \mathbf{w}_k \sim \mathcal{N}(0, \mathbf{Q}_w), \quad (104)$$

where  $\mathcal{N}(0, \mathbf{Q}_w^*)$  and  $\mathcal{N}(0, \mathbf{Q}_w)$  denote zero-mean Gaussian noise with covariance matrices for the source and primary tracking filters defined by  $\mathbf{Q}_w^*$  and  $\mathbf{Q}_w$ , respectively. Their corresponding intensities are represented by  $I_w^*$  and  $I_w$ . In both the source and primary filters, a common matrix  $\mathbf{B}_w = \text{diag}[\sigma_r^2, \sigma_\zeta^2]$  is used to ensure a fair comparison. The only differing parameters between the two tracking filters are the noise intensities. For the simulations in this section, the object follows the nonlinear transition model for a duration of  $K = 100$  time steps. The initial parameters of the object state and associated covariance are set as  $\mathbf{x}_0 = [1000 \text{ m}, 300 \text{ m/s}, 1000 \text{ m}, 0 \text{ m/s}, -3^\circ/\text{s}]^T$  and  $\mathbf{P}_0 = \text{diag}[100 \text{ m}^2, 10 \text{ m}^2/\text{s}^2, 100 \text{ m}^2, 10 \text{ m}^2/\text{s}^2, 100 \times 10^{-3} \text{ rad}^2/\text{s}^2]$ . The results obtained in this section are based on averaging 10,000 iterations of Monte Carlo (MC) simulation, using the parameter settings described in Table 1.

### 8.2 Comparative Performance Results

We investigate the performance of the proposed TL-UKF and TL-CKF algorithms in a scenario involving a single maneuvering object. The trajectory of the object is depicted in Fig. 4. Our proposed algorithms are evaluated by computing the root-mean square error (RMSE) for the position of the object in the primary tracking filter. Under the noise intensities of  $I_w = 4$  for the primary tracking filter and  $I_w^* = 1$  for the source tracking filter, performance

Table 1: Simulation Parameter Settings

Parameter	Value	Parameter	Value
$n_{\mathbf{x}}$	5	$n_{\mathbf{z}}$	2
$T_s$	1 s	$K$	100
$MC$	10,000	$\alpha$	1
$\kappa$	$-2 \rightarrow 10$	$q_1$	$0.1 \text{ m}^2/\text{s}^4$
$q_2$	$1.75 \times 10^{-2} \text{ rad}^2/\text{s}^3$	$\sigma_r$	10 m
$\sigma_\zeta$	$\sqrt{10} \times 10^{-3} \text{ rad}$	$I_{\mathbf{w}}^*$	1
$I_{\mathbf{w}}$	$0.5 \rightarrow 8$		

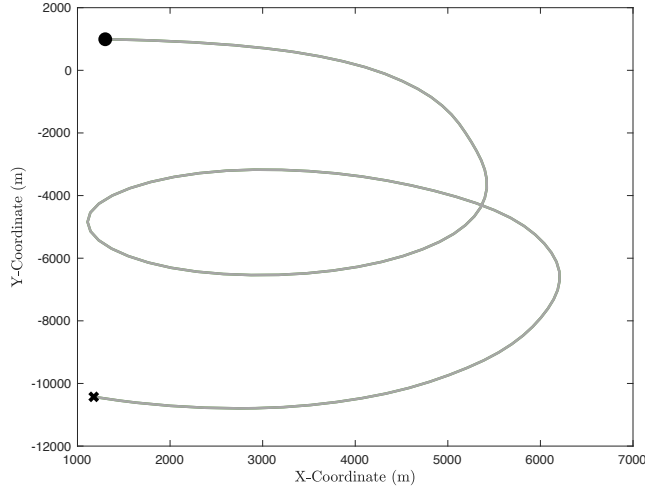


Figure 4: Object trajectory maneuvering, where  $\bullet$  indicates the initial point of the object, following the nonlinear dynamic motion model specified by the parameters in Table 1.

results in terms of RMSE for incorporating transfer learning compared to isolated filters are presented in Fig. 5. For instance, at  $k = 62$  s, the proposed third-degree TL-CKF, TL-UKF (with  $\kappa = 2$ ), and fifth-degree TL-CKF algorithms achieve RMSE values of 16.68 m, 14.39 m, and 13.56 m, respectively. In contrast, at the same time step, the isolated filters, third-degree CKF, UKF (with  $\kappa = 2$ ), and fifth-degree CKF, obtain RMSE values of 18.03 m, 17.03 m, and 16.87 m, respectively. As illustrated in Fig. 5, the proposed algorithms that incorporate transfer learning significantly outperform the isolated traditional filters.

However, as seen from the RMSE results in Fig. 5, the proposed TL-UKF algorithm (with  $\kappa = -2$ ) exhibits poorer performance at certain time steps, specifically  $k = \{8, 45, 62\}$  s. For example, the isolated UKF (with  $\kappa = -2$ ), at  $k = 62$  s, has an RMSE of 24.87 m, whereas the proposed TL-UKF obtains an RMSE of 27.48 m. This discrepancy can be attributed to the numerical instability issue, discussed in Section 6, that arises when choosing negative values of  $\kappa$ . The proposed TL-UKF algorithm is significantly more sensitive to the numerical instability issue compared to the isolated UKF due to the reliance on transfer learning, particularly in the context of predicted observations. The choice of the negative value of  $\kappa$  can lead to inaccurate approximations when applying the UT via (64)-(69) in the predict observation step of the TL-UKF framework. For this reason, leveraging inaccurate approximations from the source tracking filter can distort the estimation process in the primary tracking filter, yielding poorer estimation accuracy.

### 8.3 Impact of Varying $\kappa$ and Noise Intensity

The overall RMSE results under varying values of noise intensity,  $I_{\mathbf{w}} = 0.5 \rightarrow 8$ , in the primary tracking filter when the noise intensity value of the source filter is fixed at  $I_{\mathbf{w}}^* = 1$  are plotted in Fig. 6. As expected, the overall performance using transfer learning (dotted lines) shows a significant improvement compared to that using isolated



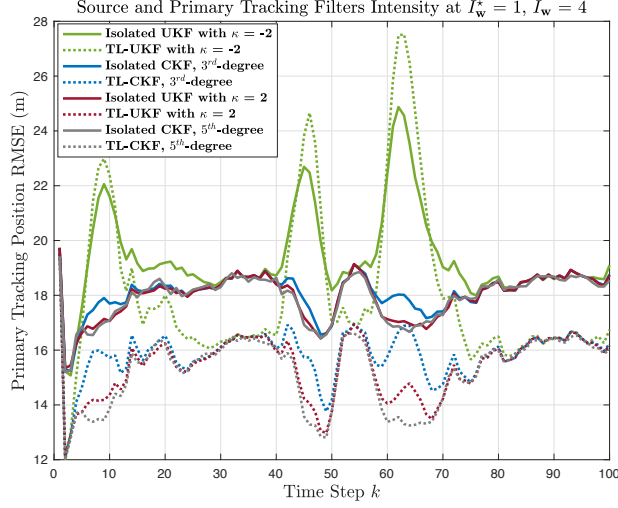


Figure 5: RMSE curves of incorporated transfer learning to the UKF and the CKF alongside the corresponding isolated filters under noise intensities  $I_w = 4$  and  $I_w^* = 1$ .

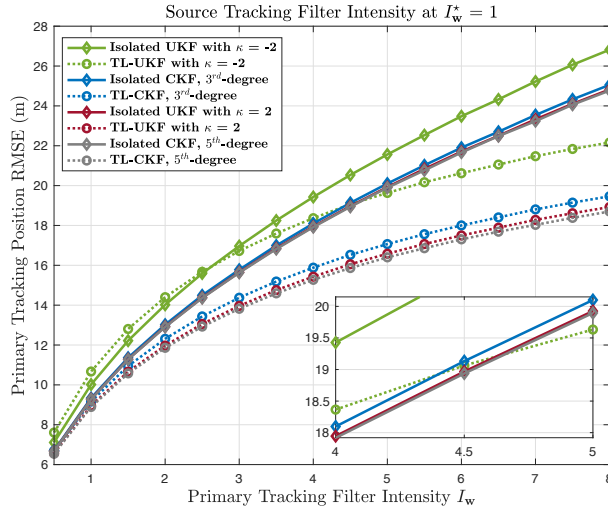


Figure 6: Performance comparison of TL-UKF, TL-CKF, and their isolated filter algorithms across varying levels of the primary filter noise intensity  $I_w$ .

filters (solid lines). For instance, the proposed algorithm TL-UKF (with  $\kappa = 2$ ) achieves an RMSE of 18.92 m under a noise intensity value of  $I_w = 8$ , while the isolated UKF achieves an equivalent RMSE of 18.96 m with a lower noise intensity value of  $I_w = 4.5$ . This indicates that the proposed algorithm is capable of tracking the object with comparable estimation accuracy, even when faced with a noise intensity in the primary tracking filter that is approximately 3.5 greater. Note that, as the noise intensity  $I_w$  increases, the difference in terms of RMSE performance between the isolated filters (solid lines) and the proposed algorithms (dotted lines), i.e., third-degree TL-CKF, TL-UKF (with  $\kappa = 2$ ), and fifth-degree TL-CKF, increases, as shown in Fig. 6.

To demonstrate the effect of the scaling parameter  $\kappa$  on the overall tracking performance, we simulated our proposed algorithms, a variant of the MVF (Measurement Vector Fusion) filter, and the isolated filters with varying values of  $\kappa = -2 \rightarrow 10$ . In the ideal MVF, the measurements from the source and primary sensors, i.e.,  $\mathbf{z}^*$  and  $\mathbf{z}$ , respectively,

are fused according to [17]

$$\tilde{\mathbf{z}}_k = \mathbf{z}_k + \mathbf{Q}_w(\mathbf{Q}_w + \mathbf{Q}_w^*)^{-1}(\mathbf{z}_k^* - \mathbf{z}_k), \quad (105)$$

$$\tilde{\mathbf{Q}}_w = [\mathbf{Q}_w^{-1} + (\mathbf{Q}_w^*)^{-1}]^{-1}, \quad (106)$$

where  $\tilde{\mathbf{z}}$  denotes the minimum mean square estimate and  $\tilde{\mathbf{Q}}_w$  is the associated covariance matrix. The fused measurement vector  $\tilde{\mathbf{z}}$  is tracked to obtain an estimate of the state vector. In [18], the MVF was shown to outperform state vector fusion, in which the filtered state vectors of the two sensors are fused into a new estimate of the state vector [30]. In particular, a reduction in the covariance of the filtered state vector is achieved by applying MVF. Since there is a one-step delay in transferring information from the source to the primary sensor, Eqs. (105) and (106) cannot be implemented in practice. Therefore, following [14], we have implemented a variant of MVF, in which the *predicted* observation  $\eta_k^*$  is transferred to the primary sensor at time  $k$ .

As seen in Table 2, as the value of  $\kappa$  increases, the position RMSE of the primary tracking filter decreases for tracking with transfer learning and approaches that of the modified MVF. Note that the RMSE performance of TL-UKF (with  $\kappa = 8$ ) achieves values of 8.8670 m, 15.1862 m, and 18.5899 m compared to 8.8712 m, 15.1938 m, and 18.5959 m when employing the MVF approach under noise intensities  $I_w = 1, 4, \text{ and } 8$ , respectively, as given in Table 2. Equivalently, the RMSE values of the third-degree and fifth-degree TL-CKF are lower in comparison with those of the MVF approach under the same conditions. The obtained RMSE values indicate that tracking with transfer learning marginally outperforms the MVF filter. As noted in [14], the MVF approach requires the strong modeling assumption of conditional independence between  $\mathbf{z}^*$  and  $\mathbf{z}$ , conditioned on a common  $\mathbf{x}$ . This assumption may be difficult to justify in applications and is not required in the BTL approach proposed here.

Table 2: Primary Tracking Filter Position RMSE (m)

Filter	$I_w = 1$			$I_w = 4$			$I_w = 8$		
	Isolated	MVF	BTLF	Isolated	MVF	BTLF	Isolated	MVF	BTLF
UKF, $\kappa = -2$	10.0168	10.6832	10.6702	19.4272	18.3809	18.3650	26.8175	22.1719	22.1621
UKF, $\kappa = -1$	9.4626	9.5122	9.5031	18.3909	16.5208	16.5082	25.4693	20.1826	20.1733
UKF, $\kappa = 1$	9.2969	9.0288	9.0221	17.9884	15.6000	15.5895	24.8919	19.1282	19.1195
UKF, $\kappa = 2$	9.2839	8.9564	8.9503	17.9451	15.4398	15.4299	24.8237	18.9328	18.9244
UKF, $\kappa = 3$	9.2819	8.9167	8.9111	17.9299	15.3440	15.3346	24.7972	18.8115	18.8034
UKF, $\kappa = 4$	9.2848	8.8942	8.8890	17.9283	15.2838	15.2747	24.7914	18.7319	18.7241
UKF, $\kappa = 5$	9.2900	8.8815	8.8765	17.9337	15.2449	15.2362	24.7965	18.6777	18.6704
UKF, $\kappa = 6$	9.2962	8.8747	8.8701	17.9428	15.2196	15.2114	24.8076	18.6403	18.6334
UKF, $\kappa = 7$	9.3029	8.8717	8.8673	17.9539	15.2035	15.1956	24.8219	18.6141	18.6076
UKF, $\kappa = 8$	9.3097	8.8712	8.8670	17.9659	15.1938	15.1862	24.8380	18.5959	18.5899
UKF, $\kappa = 9$	9.3165	8.8724	8.8684	17.9784	15.1885	15.1812	24.8549	18.5836	18.5780
UKF, $\kappa = 10$	9.3230	8.8747	8.8708	17.9909	15.1865	15.1795	24.8721	18.5755	18.5704
CKF, 3 <sup>rd</sup> -degree	9.3371	9.1727	9.1651	18.0973	15.8928	15.8815	25.0541	19.4727	19.4637
CKF, 5 <sup>th</sup> -degree	9.2784	8.8973	8.8922	17.9178	15.2803	15.2728	24.7675	18.7063	18.6989

The tracking performance plotted in Fig. 7 shows that the isolated UKF (with  $\kappa > 0$ ) outperforms the isolated third-degree CKF; however, the isolated UKF does not surpass the performance of the isolated fifth-degree CKF. On the other hand, the proposed TL-UKF achieves superior performance compared to the fifth-degree CKF where  $\kappa > 4$ . We observe from Fig. 7 that the RMSE performances of isolated UKF and TL-UKF with  $\kappa = 0$  are identically equal to those of the third-degree isolated CKF and TL-CKF, respectively. These identical performance results are expected due to the consideration of the third-degree CKF as a special case of the UKF (with  $\kappa = 0$ ), as discussed in Section 6.

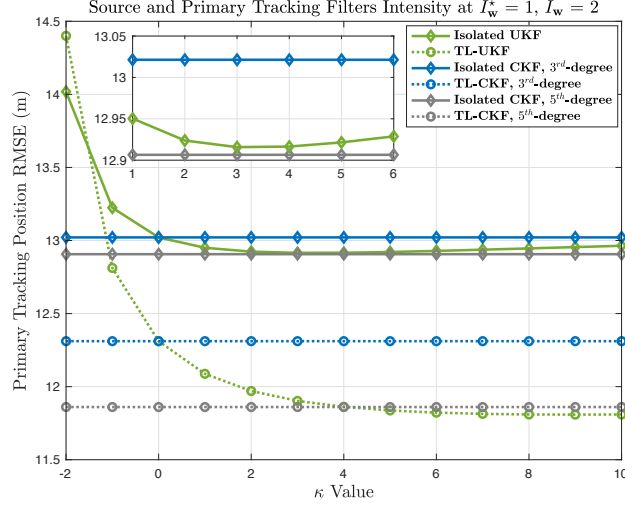


Figure 7: Performance comparison under noise intensities,  $I_w^* = 1$  and  $I_w = 2$  as a function of  $\kappa$  for the proposed transfer learning filters (dotted lines) and the corresponding isolated filters (solid lines).

## 9 Conclusion

We proposed tracking algorithms for a pair of tracking systems that incorporate Bayesian transfer learning into the UKF, third-degree CKF, and fifth-degree CKF. Our simulation results showed a significant improvement in overall tracking accuracy of the proposed algorithms compared to the corresponding isolated filters. Furthermore, by adopting the BTLF approach, a marginal improvement in overall accuracy performance compared to a version of measurement vector fusion was obtained. This is significant because measurement vector fusion is known to outperform other fusion methods in multi-sensor systems, including state vector fusion [18]. On the other hand, the MVF approach requires a strong modeling assumption that may not be justified in some applications (see Section 8.3).

We also investigated the impact of choosing the scaling parameter  $\kappa$  value for the isolated UKF and TL-UKF. For high-dimensional systems, with  $\kappa = 3 - n_x$ , a negative value of  $\kappa$  might be selected that introduces the numerical stability issue for the UKF. Interestingly, the TL-UKF turns out to be highly sensitive to the value of  $\kappa$ , more so than the isolated UKF. Our simulation results showed that the performance of TL-UKF surpasses that of the fifth-degree TL-CKF when  $\kappa > 5$ . Such performance cannot be achieved with the isolated UKF. In this paper, the BTLF is approximated via locally approximate nonlinear filters. As future work, it would be of interest to investigate approximation of the BTLF using globally approximate approaches for tracking nonlinear trajectories.

## A TL-UKF Algorithms

The TL-UKF learning and tracking algorithms, based on the equations derived in Section 5, are given in Algorithms 1 and 2, respectively. Learning and tracking algorithms for the TL-CKF based on the equations of Section 7, can be formulated similarly.

## B Bayesian Transfer Learning Derivation

### B.1 Source Tracking Filter

The overall posterior density of the state object  $\mathbf{x}_k^*$  and the predicted observation  $\boldsymbol{\eta}_{k+1}^*$  in (9) given the measurement set  $\mathbf{z}_{1:k}^*$  is derived by

$$p(\mathbf{x}_k^*, \boldsymbol{\eta}_{k+1}^* | \mathbf{z}_{1:k}^*) = \frac{p(\mathbf{x}_k^*, \boldsymbol{\eta}_{k+1}^*, \mathbf{z}_{1:k}^*)}{p(\mathbf{z}_{1:k}^*)}. \quad (107)$$

The joint expression  $p(\mathbf{x}_k^*, \boldsymbol{\eta}_{k+1}^*, \mathbf{z}_{1:k}^*)$  in the numerator of (107) is given by

$$p(\mathbf{x}_k^*, \boldsymbol{\eta}_{k+1}^*, \mathbf{z}_{1:k}^*) = p(\mathbf{x}_k^* | \boldsymbol{\eta}_{k+1}^*, \mathbf{z}_{1:k}^*)p(\boldsymbol{\eta}_{k+1}^* | \mathbf{z}_{1:k}^*)p(\mathbf{z}_{1:k}^*), \quad (108)$$

**Algorithm 1** TL-UKF Source Tracking Algorithm**Inputs:**  $\mathbf{z}_k^*$ ,  $\hat{\mathbf{x}}_{k-1|k-1}^*$ ,  $\mathbf{P}_{k-1|k-1}^*$ **Outputs:**  $\hat{\mathbf{x}}_{k|k}^*$ ,  $\mathbf{P}_{k|k}^*$ ,  $\hat{\boldsymbol{\eta}}_{k+1|k}^*$ ,  $\mathbf{P}_{\boldsymbol{\eta},k+1|k}^*$ **Prediction Step:**Apply (51) – (56) to compute  $\boldsymbol{\mathcal{X}}_{j,k-1|k-1}^*$ ,  $W_{j,k}^*$ ,  $\hat{\mathbf{x}}_{k|k-1}^*$ ,  $\mathbf{P}_{k|k-1}^*$ , and  $\boldsymbol{\mathcal{X}}_{j,k|k-1}^*$  for  $j=0, \dots, 2n_{\mathbf{x}}$ .**Update Step:**Apply (58) – (62) to compute  $\hat{\mathbf{z}}_{k|k-1}^*$ ,  $\mathbf{P}_{\mathbf{z},k|k-1}^*$ ,  $\mathbf{P}_{\mathbf{x}\mathbf{z},k|k-1}^*$ ,  $\mathbf{K}_k^*$ ,  $\hat{\mathbf{x}}_{k|k}^*$ , and  $\mathbf{P}_{k|k}^*$ .**Predicted Observation Step:**Apply (64) – (69) to compute  $\boldsymbol{\mathcal{X}}_{j,k|k}^*$ ,  $\boldsymbol{\mathcal{X}}_{j,k+1|k}^*$ ,  $\hat{\boldsymbol{\eta}}_{k+1|k}^*$ ,  $\mathbf{P}_{\boldsymbol{\eta},k+1|k}^*$  for  $j=0, \dots, 2n_{\mathbf{x}}$ .Transfer the estimated parameters  $\hat{\boldsymbol{\eta}}_{k+1|k}^*$  and  $\mathbf{P}_{\boldsymbol{\eta},k+1|k}^*$  to the primary tracking filter.**Algorithm 2** TL-UKF Primary Tracking Algorithm**Inputs:**  $\mathbf{z}_k$ ,  $\hat{\mathbf{x}}_{k-1|k-1}$ ,  $\mathbf{P}_{k-1|k-1}$ ,  $\hat{\boldsymbol{\eta}}_{k|k-1}^*$ ,  $\mathbf{P}_{\boldsymbol{\eta},k|k-1}^*$ **Outputs:**  $\hat{\mathbf{x}}_{k|k}$ ,  $\mathbf{P}_{k|k}$ **Prediction Step:**Draw  $2n_{\mathbf{x}} + 1$  sigma points  $\boldsymbol{\mathcal{X}}_{j,k-1|k-1}$  (70).Calculate  $W_{j,k}$ ,  $\hat{\mathbf{x}}_{k|k-1}$ ,  $\mathbf{P}_{k|k-1}$ , and  $\boldsymbol{\mathcal{X}}_{j,k|k-1}$  for  $j=0, \dots, 2n_{\mathbf{x}}$  using (73) – (76).**Update Step:**Calculate  $\hat{\boldsymbol{\eta}}_{k|k-1}$ ,  $\mathbf{P}_{\boldsymbol{\eta},k|k-1}$ ,  $\mathbf{P}_{\mathbf{x}\boldsymbol{\eta},k|k-1}$ ,  $\mathbf{K}_k^\eta$ ,  $\hat{\mathbf{x}}_{k|k-1}^\eta$ ,  $\mathbf{P}_{k|k-1}^\eta$  using (77) – (81).Draw  $2n_{\mathbf{x}} + 1$  sigma points  $\boldsymbol{\mathcal{X}}_{j,k|k-1}^\eta$  (85).Calculate  $\hat{\mathbf{z}}_{k|k-1}$ ,  $\mathbf{P}_{\mathbf{z},k|k-1}$ ,  $\mathbf{K}_k$ ,  $\hat{\mathbf{x}}_{k|k}$ ,  $\mathbf{P}_{k|k}$  using (86) – (90)

where  $p(\mathbf{x}_k^* | \boldsymbol{\eta}_{k+1}^*, \mathbf{z}_{1:k}^*) = p(\mathbf{x}_k^* | \mathbf{z}_{1:k}^*)$ , as the state posterior density at the current time step  $k$  is independent of the predicted observation of the next time step  $k+1$ . By substituting the joint expression from (108) into (107), the overall posterior density can now be rewritten as

$$p(\mathbf{x}_k^*, \boldsymbol{\eta}_{k+1}^* | \mathbf{z}_{1:k}^*) = p(\mathbf{x}_k^* | \mathbf{z}_{1:k}^*) p(\boldsymbol{\eta}_{k+1}^* | \mathbf{z}_{1:k}^*). \quad (109)$$

**B.2 Primary Tracking Filter**

The overall posterior density of the state object  $\mathbf{x}_k$  given the set of transferred predicted observations  $\boldsymbol{\eta}_{1:k}^*$  and observed measurements  $\mathbf{z}_{1:k}$  up to time step  $k$  is derived as

$$p(\mathbf{x}_k | \mathbf{z}_{1:k}, \boldsymbol{\eta}_{1:k}^*) = \frac{p(\mathbf{x}_k, \mathbf{z}_{1:k}, \boldsymbol{\eta}_{1:k}^*)}{p(\mathbf{z}_{1:k}, \boldsymbol{\eta}_{1:k}^*)}. \quad (110)$$

The numerator in (110) can be obtained as

$$\begin{aligned} & p(\mathbf{x}_k, \mathbf{z}_{1:k}, \boldsymbol{\eta}_{1:k}^*) \\ &= p(\mathbf{z}_k | \mathbf{x}_k, \mathbf{z}_{1:k-1}, \boldsymbol{\eta}_{1:k}^*) p(\boldsymbol{\eta}_k^* | \mathbf{x}_k, \mathbf{z}_{1:k-1}, \boldsymbol{\eta}_{1:k-1}^*) \\ & \quad \cdot p(\mathbf{x}_k | \mathbf{z}_{1:k-1}, \boldsymbol{\eta}_{1:k-1}^*) p(\mathbf{z}_{1:k-1}, \boldsymbol{\eta}_{1:k-1}^*). \end{aligned} \quad (111)$$

Under the assumption that the measurements and the transferred predicted observations are conditionally independent given the object state  $\mathbf{x}_k$ , the joint density in (111) can be simplified as

$$\begin{aligned} & p(\mathbf{x}_k, \mathbf{z}_{1:k}, \boldsymbol{\eta}_{1:k}^*) = p(\mathbf{z}_k | \mathbf{x}_k) p(\boldsymbol{\eta}_k^* | \mathbf{x}_k) \\ & \quad \cdot p(\mathbf{x}_k | \mathbf{z}_{1:k-1}, \boldsymbol{\eta}_{1:k-1}^*) p(\mathbf{z}_{1:k-1}, \boldsymbol{\eta}_{1:k-1}^*), \end{aligned} \quad (112)$$

and the denominator in (110) can be factorized as

$$\begin{aligned} & p(\mathbf{z}_{1:k}, \boldsymbol{\eta}_{1:k}^*) = p(\mathbf{z}_k, \mathbf{z}_{1:k-1}, \boldsymbol{\eta}_{1:k}^*) \\ &= p(\mathbf{z}_k | \mathbf{z}_{1:k-1}, \boldsymbol{\eta}_{1:k}^*) p(\boldsymbol{\eta}_k^* | \mathbf{z}_{1:k-1}, \boldsymbol{\eta}_{1:k-1}^*) p(\mathbf{z}_{1:k-1}, \boldsymbol{\eta}_{1:k-1}^*). \end{aligned} \quad (113)$$

The overall posterior density can be obtained by substituting the simplified numerator from (112) and the factorized denominator from (113) into (110) as

$$\begin{aligned} p(\mathbf{x}_k | \mathbf{z}_{1:k}, \boldsymbol{\eta}_{1:k}^*) &= \frac{p(\mathbf{z}_k | \mathbf{x}_k) p(\boldsymbol{\eta}_k^* | \mathbf{x}_k) p(\mathbf{x}_k | \mathbf{z}_{1:k-1}, \boldsymbol{\eta}_{1:k-1}^*)}{p(\mathbf{z}_k | \mathbf{z}_{1:k-1}, \boldsymbol{\eta}_{1:k}^*) p(\boldsymbol{\eta}_k^* | \mathbf{z}_{1:k-1}, \boldsymbol{\eta}_{1:k-1}^*)} \end{aligned} \quad (114)$$

$$= \frac{p(\mathbf{z}_k | \mathbf{x}_k) p(\mathbf{x}_k | \mathbf{z}_{1:k-1}, \boldsymbol{\eta}_{1:k}^*)}{p(\mathbf{z}_k | \mathbf{z}_{1:k-1}, \boldsymbol{\eta}_{1:k}^*)}, \quad (115)$$

where the second term in the numerator of (115) is referred to the transfer learning state posterior density and is given by

$$p(\mathbf{x}_k | \mathbf{z}_{1:k-1}, \boldsymbol{\eta}_{1:k}^*) = \frac{p(\boldsymbol{\eta}_k^* | \mathbf{x}_k) p(\mathbf{x}_k | \mathbf{z}_{1:k-1}, \boldsymbol{\eta}_{1:k-1}^*)}{p(\boldsymbol{\eta}_k^* | \mathbf{z}_{1:k-1}, \boldsymbol{\eta}_{1:k-1}^*)}. \quad (116)$$

## References

- [1] O. Alotaibi and B. L. Mark, "Object tracking incorporating transfer learning into an unscented Kalman filter," in *Proc. 58th Annu. Conf. Inf. Sci. Syst. (CISS)*, Princeton, NJ, 2024, pp. 1–6.
- [2] H. Kushner, "Approximations to optimal nonlinear filters," *IEEE Trans. Autom. Control*, vol. 12, no. 5, pp. 546–556, 1967.
- [3] S. J. Julier and J. K. Uhlmann, "A new extension of the Kalman filter to nonlinear systems," in *Proc. Signal Process., Sensor Fusion, Target Recognit. VI*, vol. 3068, 1997, pp. 182–193.
- [4] I. Arasaratnam and S. Haykin, "Cubature Kalman filters," *IEEE Trans. Autom. Control*, vol. 54, no. 6, pp. 1254–1269, 2009.
- [5] S. J. Pan and Q. Yang, "A survey on transfer learning," *IEEE Trans. Knowl. Data Eng.*, vol. 22, no. 10, pp. 1345–1359, 2009.
- [6] B. Li, Q. Yang, and X. Xue, "Transfer learning for collaborative filtering via a rating-matrix generative model," in *Proc. 26th Annu. Int. Conf. Mach. Learn.*, 2009, pp. 617–624.
- [7] E. Grolman, A. Bar, B. Shapira, L. Rokach, and A. Dayan, "Utilizing transfer learning for in-domain collaborative filtering," *Knowl. Base. Syst.*, vol. 107, pp. 70–82, 2016.
- [8] J. Xuan, J. Lu, and G. Zhang, "Bayesian transfer learning: An overview of probabilistic graphical models for transfer learning," *arXiv:2109.13233*, 2021.
- [9] A. Karbalayghareh, X. Qian, and E. R. Dougherty, "Optimal Bayesian transfer learning," *IEEE Trans. Signal Process.*, vol. 66, no. 14, pp. 3724–3739, 2018.
- [10] X. Wu, J. H. Manton, U. Aickelin, and J. Zhu, "A Bayesian approach to (online) transfer learning: Theory and algorithms," *Artif. Intell.*, vol. 324, p. 103991, 2023.
- [11] M. Papež and A. Quinn, "Transferring model structure in Bayesian transfer learning for Gaussian process regression," *Knowl. Base. Syst.*, vol. 251, p. 108875, 2022.
- [12] A. Karbalayghareh, X. Qian, and E. R. Dougherty, "Optimal Bayesian transfer regression," *IEEE Signal Process. Lett.*, vol. 25, no. 11, pp. 1655–1659, 2018.
- [13] Q. Wang, F. Chen, J. Yang, W. Xu, and M.-H. Yang, "Transferring visual prior for online object tracking," *IEEE Trans. Image Process.*, vol. 21, no. 7, pp. 3296–3305, 2012.
- [14] C. Foley and A. Quinn, "Fully probabilistic design for knowledge transfer in a pair of Kalman filters," *IEEE Signal Process. Lett.*, vol. 25, no. 4, pp. 487–490, 2017.
- [15] M. Papež and A. Quinn, "Robust Bayesian transfer learning between Kalman filters," in *Proc. IEEE 29th Int. Workshop Mach. Learn. for Signal Process. (MLSP)*, 2019, pp. 1–6.
- [16] —, "Hierarchical Bayesian transfer learning between a pair of Kalman filters," in *Proc. IET Ir. Signals Syst. Conf.*, 2021, pp. 1–5.
- [17] D. Willner, C. B. Chang, and K. P. Dunn, "Kalman filter algorithms for a multi-sensor system," in *Proc. IEEE Conf. Decis. Control Including 15th Symp. Adapt. Processes*, 1976, pp. 570–574.
- [18] J. A. Roecker and C. D. McGillem, "Comparison of two-sensor tracking methods based on state vector fusion and measurement fusion," *IEEE Trans. Aerosp. Electron. Syst.*, vol. 24, no. 4, pp. 447–449, Jul. 1988.

- 
- [19] Y. Ho and R. Lee, "A Bayesian approach to problems in stochastic estimation and control," *IEEE Trans. Autom. Control*, vol. 9, no. 4, pp. 333–339, October 1964.
- [20] B. Ristic, S. Arulampalam, and N. Gordon, *Beyond the Kalman Filter: Particle Filters for Tracking Applications*. Norwood, MA: Artech House, 2004.
- [21] N. J. Gordon, D. J. Salmond, and A. F. M. Smith, "Novel approach to nonlinear/non-Gaussian Bayesian state estimation," *Proc. Inst. Elect. Eng. F*, vol. 140, no. 2, pp. 107–113, April 1993.
- [22] M. S. Arulampalam, S. Maskell, N. Gordon, and T. Clapp, "A tutorial on particle filters for online nonlinear/non-Gaussian Bayesian tracking," *IEEE Trans. Signal Process.*, vol. 50, no. 2, pp. 174–188, Feb. 2002.
- [23] E. A. Wan and R. Van Der Merwe, "The unscented Kalman filter for nonlinear estimation," in *Proc. IEEE Adaptive Syst. Signal Process., Commun., Control Symp.*, Oct. 2000, pp. 153–158.
- [24] S. Julier, J. Uhlmann, and H. F. Durrant-Whyte, "A new method for the nonlinear transformation of means and covariances in filters and estimators," *IEEE Trans. Autom. Control*, vol. 45, no. 3, pp. 477–482, March 2000.
- [25] A. Genz and B. D. Keister, "Fully symmetric interpolatory rules for multiple integrals over infinite regions with Gaussian weight," *J. Comput. Appl. Math.*, vol. 71, no. 2, pp. 299–309, 1996.
- [26] B. Jia, M. Xin, and Y. Cheng, "High-degree cubature Kalman filter," *Automatica*, vol. 49, no. 2, pp. 510–518, 2013.
- [27] L. Chang, B. Hu, A. Li, and F. Qin, "Transformed unscented Kalman filter," *IEEE Trans. Autom. Control*, vol. 58, no. 1, pp. 252–257, 2012.
- [28] S. J. Julier and J. K. Uhlmann, "Unscented filtering and nonlinear estimation," *Proc. IEEE*, vol. 92, no. 3, pp. 401–422, March 2004.
- [29] Y. Bar-Shalom, X. R. Li, and T. Kirubarajan, *Estimation with Applications to Tracking and Navigation: Theory Algorithms and Software*. New York, NY: Wiley, 2001.
- [30] Y. Bar-Shalom and L. Campo, "The effect of the common process noise on the two-sensor fused-track covariance," *IEEE Trans. Aerosp. Electron. Syst.*, vol. 22, pp. 803–805, Nov. 1986.